

Forced subduction initiation within the Neotethys: An example from the mid-Cretaceous Wuntho-Popa arc in Myanmar

Liyun Zhang^{1,†}, Weiming Fan^{1,2,§}, Lin Ding^{1,2,§}, Alex Pullen^{3,§}, Mihai N. Ducea^{4,5,§}, Jinxiang Li^{1,§}, Chao Wang^{1,§}, Xiaoyan Xu^{1,2,§}, and Kyaing Sein^{6,§}

¹State Key Laboratory of Tibetan Plateau Earth System, Resources and Environment, Institute of Tibetan Plateau Research, Chinese Academy of Sciences, Beijing 100101, China

²University of Chinese Academy of Sciences, Beijing 100049, China

³Department of Environmental Engineering and Earth Sciences, Clemson University, Clemson, South Carolina 29634, USA

⁴Department of Geosciences, University of Arizona, Tucson, Arizona 85721, USA

⁵Universitatea Bucuresti, Facultatea de Geologie Geofizica, Str. N. Balcescu Nr1., Bucuresti 010041, Romania

⁶Myanmar Geosciences Society, Yangon, Myanmar

ABSTRACT

Despite decades of research, the mechanisms and processes of subduction initiation remain obscure, including the tectonic settings where subduction initiation begins and how magmatism responds. The Cretaceous Mawgyi Volcanics represent the earliest volcanic succession in the Wuntho-Popa arc of western Myanmar. This volcanic unit consists of an exceptionally diverse range of contemporaneously magmatic compositions which are spatially juxtaposed. Our new geochemical data show that the Mawgyi Volcanics comprise massive mid-oceanic ridge basalt (MORB)-like lavas and dikes, and subordinate island arc tholeiite and calc-alkaline lavas. The Mawgyi MORB-like rocks exhibit flat rare earth elements (REEs) patterns and are depleted in REEs, high field strength elements (except for Th) and TiO₂ concentrations relative to those of MORBs, resembling the Izu-Bonin-Mariana protoarc basalts. Our geochronological results indicate that the Mawgyi Volcanics formed between 105 and 93 Ma, coincident with formation of many Neotethyan supra-subduction zone ophiolites and intraoceanic arcs along orogenic strike in the eastern Mediterranean, Middle East, Pakistan, and Southeast Asia. Combined


with its near-equatorial paleo-latitudes constrained by previous paleomagnetic data, the Wuntho-Popa arc is interpreted as a segment of the north-dipping trans-Neotethyan subduction system during the mid-Cretaceous. Importantly, our restoration with available data provides new evidence supporting the hypothesis of a mid-Cretaceous initiation of this >8000-km-long subduction system formed by inversion of the ~E-W-trending Neotethyan oceanic spreading ridges, and that this was contemporaneous with the final breakup of Gondwana and an abrupt global plate reorganization.

INTRODUCTION

Development of the Himalayan-Tibetan orogen resulted from multiple ocean closures and terrane accretion events and culminated with the early Cenozoic India-Asia collision (Fig. 1; Kapp and DeCelles, 2019). The presence of a near-equatorial, north-dipping intraoceanic subduction zone within the Neotethys has long been proposed (e.g., Proust et al., 1984; Searle et al., 1987), but remnants of which are relatively spatially localized and/or disputed. For example, island arc relicts may be preserved along the Yarlung-Tsangpo suture between Indian and Asian affinity rocks as distributed ophiolitic fragments (e.g., Abrajevitch et al., 2005; Aitchison et al., 2000, 2007). Abundant geological and geochronological studies, however, show that a majority of the Yarlung-Tsangpo ophiolites formed synchronously during the Early Cretaceous and were generated in a wide range of tectonic environments, including mid-oceanic ridge, forearc or back-arc basin, and intraoceanic arc (Dai et al., 2013; Guilmette et al., 2012; Hébert

et al., 2012; Liu et al., 2016b; Maffione et al., 2015a; Xiong et al., 2016; Zhang et al., 2019a). Recent paleomagnetic data indicate the Yarlung-Tsangpo ophiolites developed at relatively high latitudes of ~16.5°N (Huang et al., 2015), close to the southern continental margin of Asia, rather than a near-equatorial latitude (Abrajevitch et al., 2005). Some have also suggested that the ophiolites formed the basement of the Xigaze forearc basin along the southern Asian margin (Fig. 1; Laskowski et al., 2019; Orme et al., 2015; Wang et al., 2017a). The temporal association between the formation of the Yarlung-Tsangpo ophiolites and the initial breakup of East and West Gondwana has been linked to global plate reorganization during supercontinent breakup (Qian et al., 2020). Furthermore, it has been proposed that Early Cretaceous ophiolite formation occurred above a pre-existing subduction zone near the southern margin of Asia, rather than intraoceanic subduction initiation (Butler and Beaumont, 2017; Dai et al., 2013; Maffione et al., 2015b; Xiong et al., 2016; Qian et al., 2020).

The mid-Cretaceous Kohistan-Ladakh arc in the westernmost India-Asia collision zone, located between the western Himalayas and the Pamir orogen (Fig. 1), is generally interpreted as an intraoceanic arc relict (Bouilhol et al., 2013; Burg, 2011; Corfield et al., 2001; Garrido et al., 2007; Jagoutz et al., 2015, 2019; Khan et al., 1997; Mahéo et al., 2004; Petterson and Windley, 1991; Searle et al., 1999). Paleomagnetic results indicate that the Kohistan-Ladakh intraoceanic arc was isolated at near-equatorial latitudes during the mid-Late Cretaceous (Ahmad et al., 2000; Khan et al., 2009; Klootwijk et al., 1984; Zaman and Torii, 1999) and was still active at a paleolatitude of $8.1 \pm 5.6^\circ\text{N}$ until at least Paleocene time (Martin et al., 2020). The West Burma

Liyun Zhang  <https://orcid.org/0000-0003-2282-5102>

[†]Corresponding author: zly@itpcas.ac.cn.

[§]wmfan@itpcas.ac.cn (Weiming Fan); dinglin@itpcas.ac.cn (Lin Ding); apullen@clemson.edu (Alex Pullen); ducea@arizona.edu (Mihai Ducea); ljx@itpcas.ac.cn (Jinxiang Li); wangchao@itpcas.ac.cn (Chao Wang); xuxiaoyan@itpcas.ac.cn (Xiaoyan Xu); kyaingsein@gmail.com (Kyaing Sein).

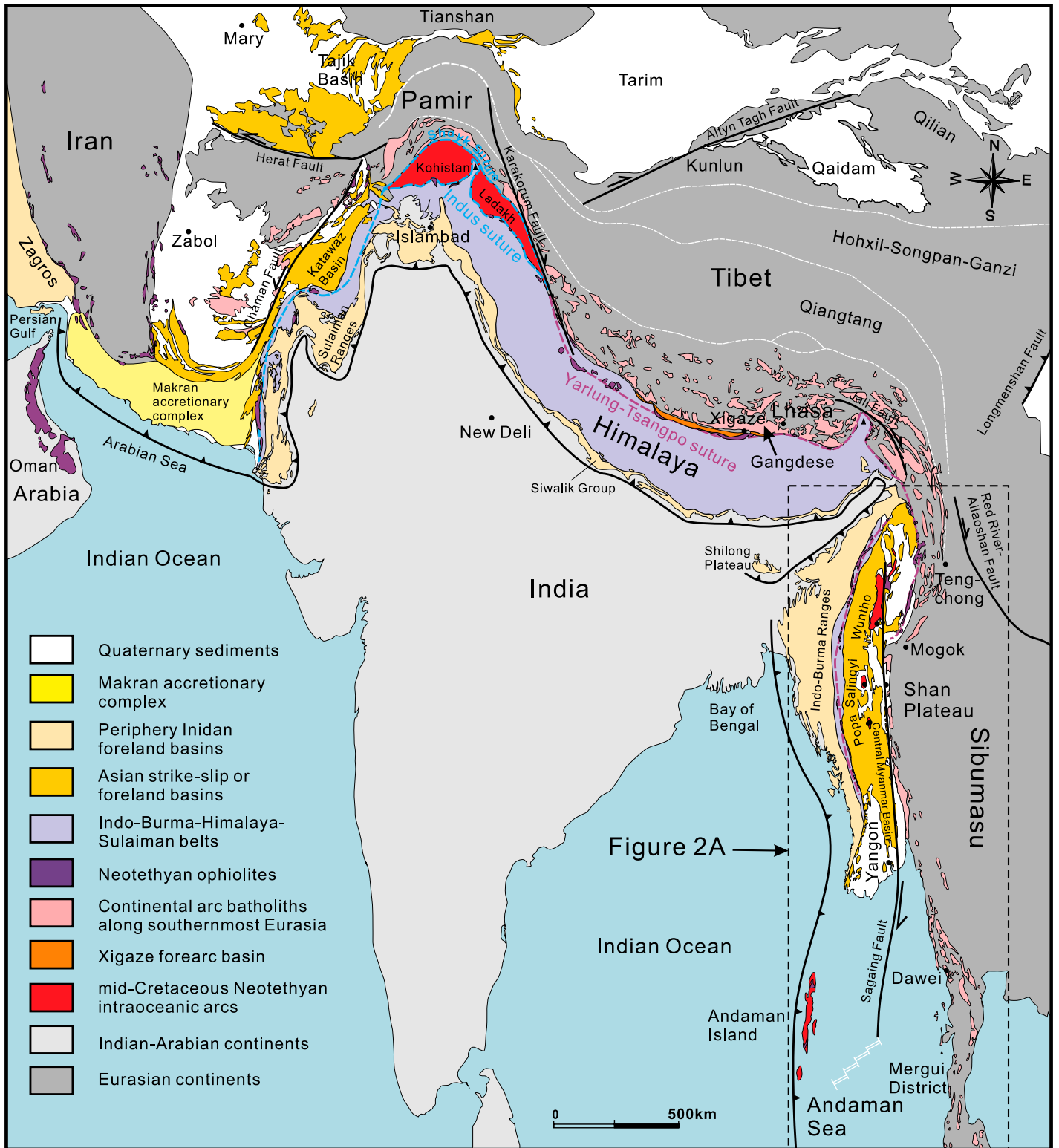


Figure 1. Schematic map of tectonics in the India-Asia collision orogen.

Terrane (WBT) is juxtaposed between the Indo-Burma ranges and the Sibumasu Terrane at the eastern edge of the India-Asia collision zone (Fig. 1). The Wuntho-Popa arc straddling the

WBT has been correlated to the mid-Cretaceous intraoceanic Andaman-Woyla arcs (Li et al., 2020b; Mitchell, 1993; Pedersen et al., 2010; Plunder et al., 2020) or the Incetrus arc (Fig. 1;

Hall, 2012, Sumatra). Recent paleomagnetic data from igneous and sedimentary rocks indicate that the Wuntho-Popa arc was located at near-equatorial latitudes during the mid-Cretaceous

to the mid-Eocene, and was disparate from the southern margin of Asia at that time (Westerweel et al., 2019). Alternatively, the Wuntho-Popa arc is simply considered as the eastward continuation of the Gangdese continental arc because they both exhibit similar isotopic signatures of juvenile crust (Li et al., 2020a; Lin et al., 2019; Wang et al., 2014; Zhang et al., 2019b).

The synchronous construction of the Kohistan-Ladakh arc and the Wuntho-Popa arc along the near-equatorial latitudes favors a scenario in which there was an active trans-Neotethyan intraoceanic subduction system during the mid-Cretaceous (e.g., Jagoutz et al., 2015; Westerweel et al., 2019). A scenario in which there were two north-dipping subduction zones within the Neotethys during the mid-Cretaceous can better account for the very rapid northward drift of the Indian plate during the Late Cretaceous to early Eocene time (Gibbons et al., 2015; Jagoutz et al., 2015; van Hinsbergen et al., 2011). However, if valid this scenario also raises the questions about where and how the intraoceanic subduction system began and how magmatism responded to build these juvenile island arcs that are presently >3000 km apart (Fig. 1). The geochemistry and petrology of the Wuntho-Popa volcanic rocks associated with new paleomagnetic constraints (Westerweel et al., 2019) have not yet been studied from a petrological perspective, but may potentially record the protoarc magmatism associated with the earliest stage of intraoceanic subduction, like the Izu-Bonin-Mariana (IBM) protoarc (Arculus et al., 2015; Ishizuka et al., 2011a; Reagan et al., 2010, 2019; Shervais et al., 2019).

Many ophiolites from the eastern Mediterranean to the Middle East mostly formed in a supra-subduction zone (SSZ) during the mid-Cretaceous and have been generally ascribed to intraoceanic subduction initiation within the Neotethys (e.g., Dilek and Furnes, 2011; Dilek and Thy, 2009; Guilmette et al., 2018; Maffione et al., 2017; Moghadam and Stern, 2015; Searle et al., 2015; van Hinsbergen et al., 2016, 2020). An overall reassessment of the tectonic settings for temporal coincidence between eastern Mediterranean-Middle East SSZ ophiolites and the Kohistan-Ladakh-Wuntho-Popa-Andaman-Woyla island arcs is thus necessary for explaining their origin. This study presents new geochemical and geochronological constraints for the Wuntho-Popa arc and aims to better understand subduction initiation within the Neotethys. It is also unclear what geodynamic processes were responsible for subduction initiation within the Neotethys during the mid-Cretaceous. We then speculate about potential causal links between intraoceanic subduction initiation and global plate reorganization related to final breakup of Gondwana during the mid-Cretaceous.

GEOLOGICAL BACKGROUND

The West Burma Terrane (WBT) is presently located above a hyper-oblique subduction zone where the Indian plate (probably both continental and oceanic crust) is being subducted beneath the Indo-Burma ranges in the west (Zhang et al., 2020, 2021; Zheng et al., 2020), and the Sagaing Fault, an active large-scale dextral strike-slip fault, in the east (Fig. 2A; Vigny et al., 2003). The oblique subduction results in a northward motion of the WBT relative to the Sibumasu Terrane (Gahalaut and Gahalaut, 2007; Ni et al., 1989). The western boundary of the WBT is typically delineated by either another dextral strike-slip fault (the Churachandpur-Mao Fault) or the Naga Hills-Manipur-Kalaymyo ophiolites (Fig. 2A; also referred to as the Western Belt ophiolites; Fareeduddin and Dilek, 2015; Htay et al., 2017; Liu et al., 2016a; Niu et al., 2017). The basement of the Indo-Burma ranges has been interpreted as either a microcontinent block accreted to the WBT during the Cretaceous–Eocene (Acharyya, 2015; Morley, 2012), or an accretionary-type orogen formed in situ (Fareeduddin and Dilek, 2015; Licht et al., 2018; Zhang et al., 2018; Morley et al., 2020). The Triassic rocks, including the Shwedaung and Pane Chung turbidites and Kanpetlet schists, are the oldest rocks exposed within the Indo-Burma ranges. However, the origin of these rocks remains debated with most advocating for either a Gondwanan or Cathaysian affinity (e.g., Sevastjanova et al., 2016; Yao et al., 2017; Morley et al., 2020). Geochronological data suggest that the Western Belt ophiolites formed during the Early Cretaceous (133–126 Ma; Liu et al., 2016a; Zhang et al., 2017a), and thus overlap in age with the Yarlung-Tsangpo ophiolites to the north (e.g., Dai et al., 2013; Qian et al., 2020; Xiong et al., 2016; Zhang et al., 2019a).

The Shan Plateau (Sibumasu Terrane) is composed of the Eastern Belt ophiolites (Liu et al., 2016a; Yang et al., 2012) and the Mogok-Mergui metamorphic and plutonic rocks that formed the eastern boundary of the WBT along the Sagaing Fault (Fig. 2A; Mitchell, 1992; Searle et al., 2007). The Mogok-Mergui belt has been considered as the southward continuation of the peri-Gondwanan Lhasa Terrane in Tibet (Fig. 1; Searle et al., 2007) bridged by the Tengchong Terrane (e.g., Xie et al., 2016). The Sagaing Fault is likely connected to the Andaman spreading center (Curry, 2005; Morley, 2012; Sloan et al., 2017) and has a displacement of up to 1100 km since the Neogene (Mitchell, 1993; Morley and Arboit, 2019), or ~2000 km since the late Eocene (ca. 38 Ma, Westerweel et al., 2019). The formation of the Andaman ophiolites is much younger (95–93 Ma; Pedersen et al.,

2010; Sarma et al., 2010) than those of the Yarlung-Tsangpo and the Western Belt ophiolites, but are coeval with the eastern Mediterranean and Middle East ophiolites and the Kohistan arc (e.g., Qian et al., 2020). This observation is at odds with the widely held view that the Andaman ophiolites are the southward continuation of the Western Belt ophiolites (Htay, 2017; Liu et al., 2016a; Mitchell, 1993; Niu et al., 2017; Pedersen et al., 2010). The metamorphic soles of Andaman ophiolites formed between 106 and 105 Ma (Plunder et al., 2020). This is also much younger than that of the Western Belt ophiolites in Myanmar (119–115 Ma; Liu et al., 2016a; Zhang et al., 2017a) but corresponding in age to metamorphic soles of the Oman ophiolites (104–103 Ma; Guilmette et al., 2018).

The WBT is primarily composed of the Late Cretaceous–Cenozoic Central Myanmar Basin which surrounds the Wuntho-Popa arc (Mitchell, 1993). The Wuntho-Popa arc is thought to have been the main source of detritus supplied to the poorly exposed strata of the Kabaw Formation until the mid-Eocene or later (Cai et al., 2019; Licht et al., 2018; Wang et al., 2014; Westerweel et al., 2020). The main pulse of plutonic magmatism in the Wuntho-Popa arc occurred during the mid-Cretaceous (105–89 Ma) based on zircon U-Pb ages (Fig. 2B; e.g., Gardiner et al., 2017; Li et al., 2020a; Lin et al., 2019; Mitchell et al., 2012; Zhang et al., 2017b). Zircon *in situ* Hf isotopic data indicate that the earliest Wuntho-Popa arc was entirely constructed on juvenile crust like the Gangdese arc (Li et al., 2020a; Lin et al., 2019; Wang et al., 2014). Recent paleomagnetic data for the Kanza Chaung Batholith and the Kondan Chaung Group in the Wuntho ranges suggest that the WBT was at a near-equatorial latitude at ca. 95 Ma, placing it at least 2000 km south of the Gangdese continental arc at that time (Westerweel et al., 2019). Plutonic rocks of the Wuntho-Popa arc, including gabbros, diorites, and granites, exclusively exhibit a low/medium-K geochemical signature (e.g., Li et al., 2020a). This distinctive signature renders their continental arc interpretation flawed since the high-K rocks generally define continental arcs (e.g., Ducea et al., 2015; Schmidt and Jagoutz, 2017). A thick sequence of Cretaceous volcanic rocks and clastic sedimentary rocks unconformably overlay the WBT basement in the Wuntho ranges (Fig. 3A). The poorly dated Mawgyi Volcanics have been interpreted as the oldest formation within the Cretaceous WBT sequences and are overlain by the Kondan Chaung Group (Mitchell, 1993). Pillow basalts and basaltic andesites are extensive and massive in Wuntho (Fig. 3A), and sills and dikes of similar composition are also found in Salingyi (Fig. 3B; Mitchell, 1993). The origin of the Mawgyi Volcanics has been inferred to

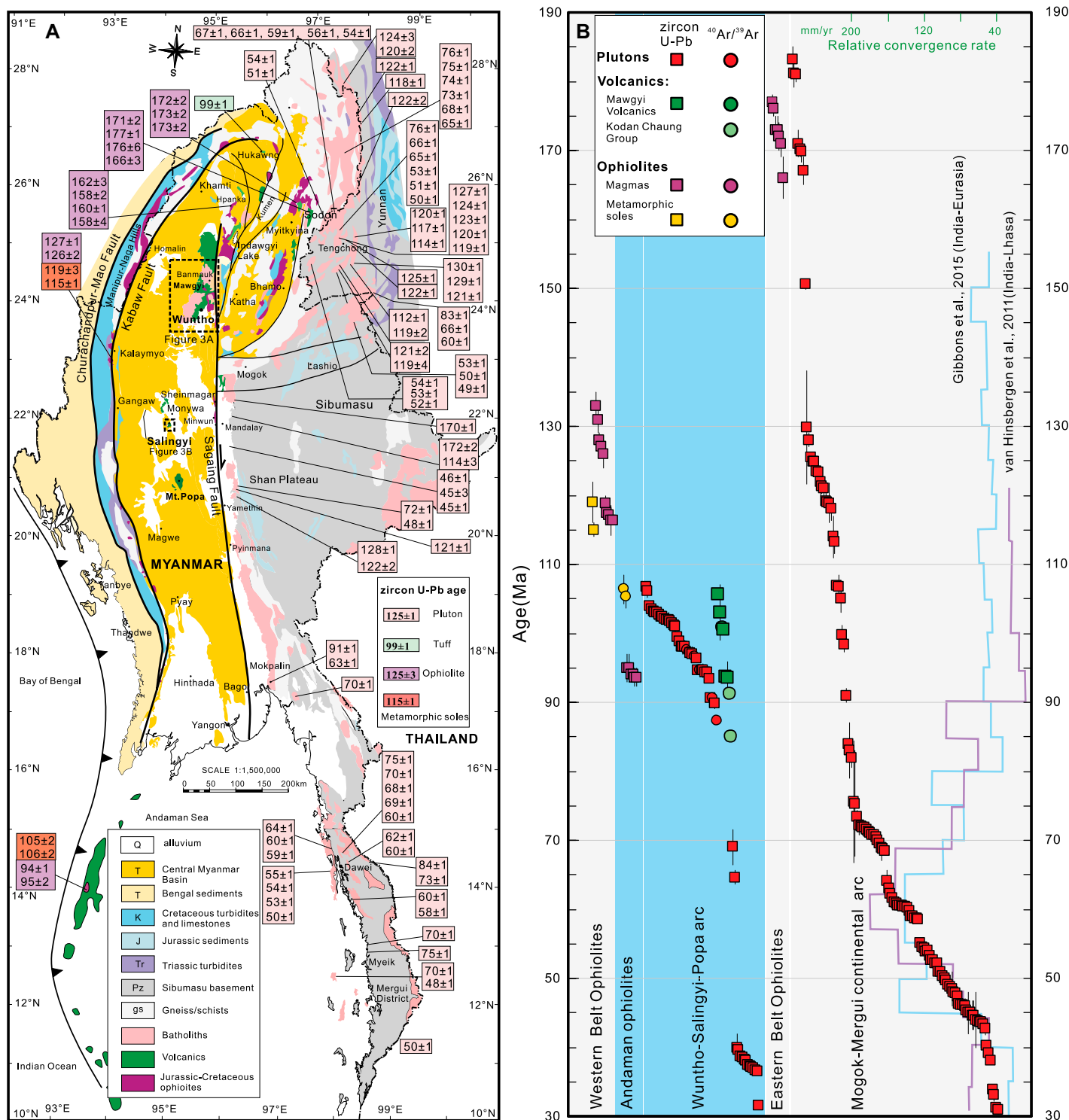


Figure 2. (A) Geological map of Myanmar and southwestern Yunnan, China after Zhang et al. (2018). Ages from the Tengchong batholiths are mainly from Xie et al. (2016); (B) Age distributions for the Western and Eastern Belt ophiolites in Myanmar and the Andaman Islands (India), and the Wuntho-Popa and Mogok-Mergui arcs (Age data, sampling locations, and references are presented in Supporting Information Table S1; see footnote 1). The convergence rates between India and Asia are from Gibbons et al. (2015) and van Hinsbergen et al. (2011). Mt.—Mount.

be associated with subduction initiation of Neotethyan oceanic lithosphere due to a reversal of subduction polarity (Mitchell, 1993), though no

geochemical data are available. Because of this, one hypothesis is that the Mawgyi Volcanics may be correlated with the Andaman ophiolites and

Woyla intraoceanic arc (Sumatra; e.g., Mitchell, 1993; Morley, 2012; Pedersen et al., 2010; Plunder et al., 2020) as part of the mid-Cretaceous

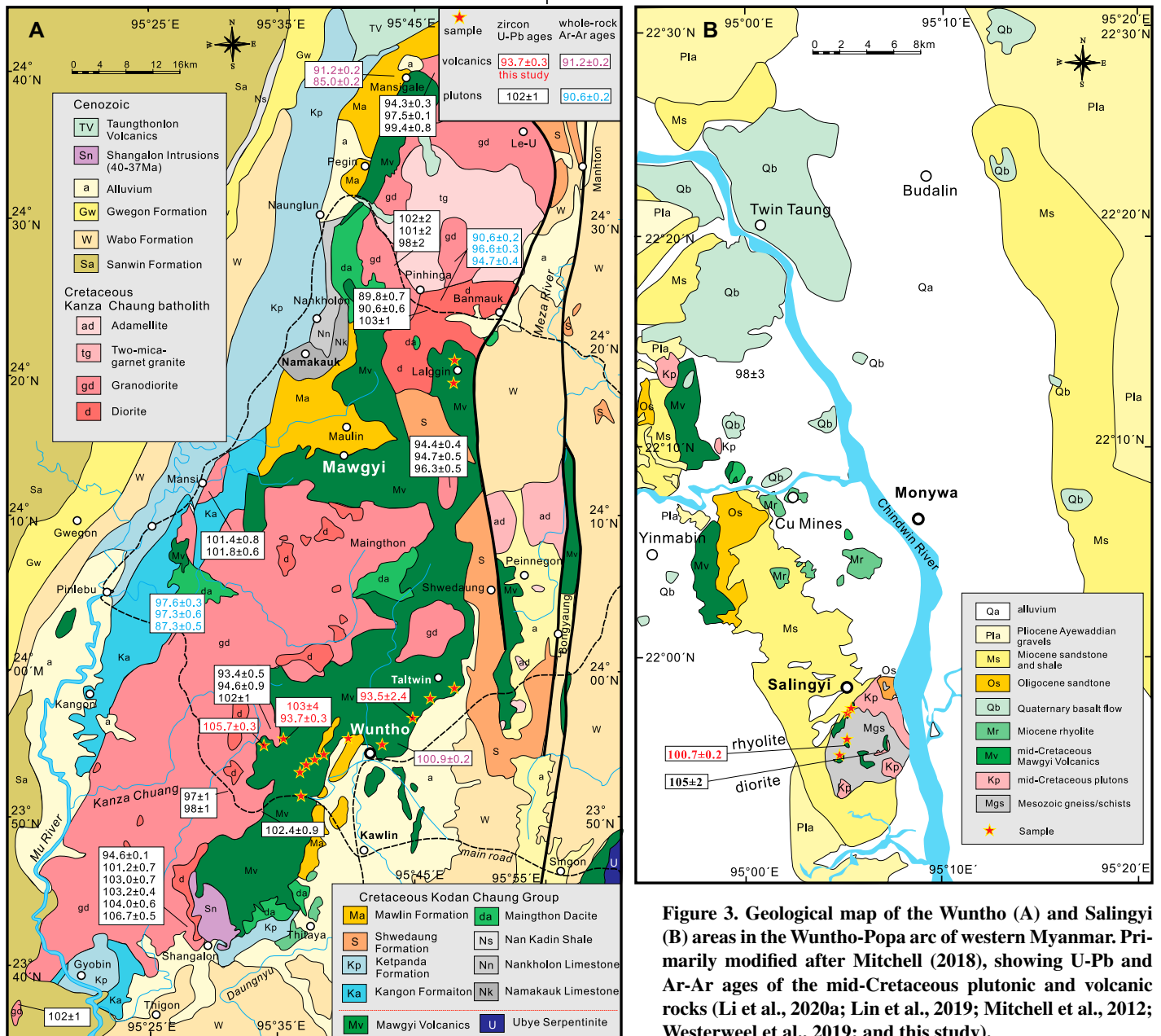


Figure 3. Geological map of the Wuntho (A) and Salingyi (B) areas in the Wuntho-Popa arc of western Myanmar. Primarily modified after Mitchell (2018), showing U-Pb and Ar-Ar ages of the mid-Cretaceous plutonic and volcanic rocks (Li et al., 2020a; Lin et al., 2019; Mitchell et al., 2012; Westerweel et al., 2019; and this study).

Incertus arc (Hall, 2012) or trans-Neotethyan intraoceanic arc (Gibbons et al., 2015; Jagoutz et al., 2015; Westerweel et al., 2019).

SAMPLES DESCRIPTION AND ANALYTICAL METHODS

Petrography

Eighty-three igneous rocks were collected from Banmauk, Wuntho, Kawlin, and Salingyi for geochronological and geochemical analysis. The widespread pillow basalts and basaltic andesites near Wuntho were sampled, and one coarse-grained gabbro was collected as

well (Fig. 3A). In addition, the doleritic and rhyolitic rocks were sampled near Salingyi (Fig. 3B). The ages of the Mawgyi Volcanics were determined, for five samples among these rocks, by zircon U-Pb geochronology. Three distinct geochemical groups can be observed within the Mawgyi Volcanics, including MORB-like rocks, island arc tholeiites, and calc-alkaline rocks. The MORB-like basalts and basaltic andesites are the most voluminous volcanic rocks in the Wuntho area. These samples include euhedral clinopyroxene and plagioclase with rare olivine within glassy matrices (Figs. 4A, 4B, 4D, and 4E). The coarse-grained gabbro has interlocked tex-

tures between clinopyroxene and plagioclase (Fig. 4C). The Salingyi dolerites, exposed as dikes, exhibit typical ophitic texture with needle-like plagioclase and fine-grained clinopyroxene altered to chlorite (Fig. 4F). The island arc tholeiitic basalts primarily contain plagioclase phenocrysts (Figs. 4G and 4H), whereas the basaltic andesite have coarse-grained, euhedral hornblende and plagioclase (Fig. 4I). The Wuntho island arc calc-alkaline rocks have plagioclase and minor fresh olivine phenocrystal clasts (Fig. 4J), and occasionally contain glomerocrysts of olivine, clinopyroxene, and plagioclase, and opaque minerals are common (Fig. 4K). The calc-alkaline dolerites

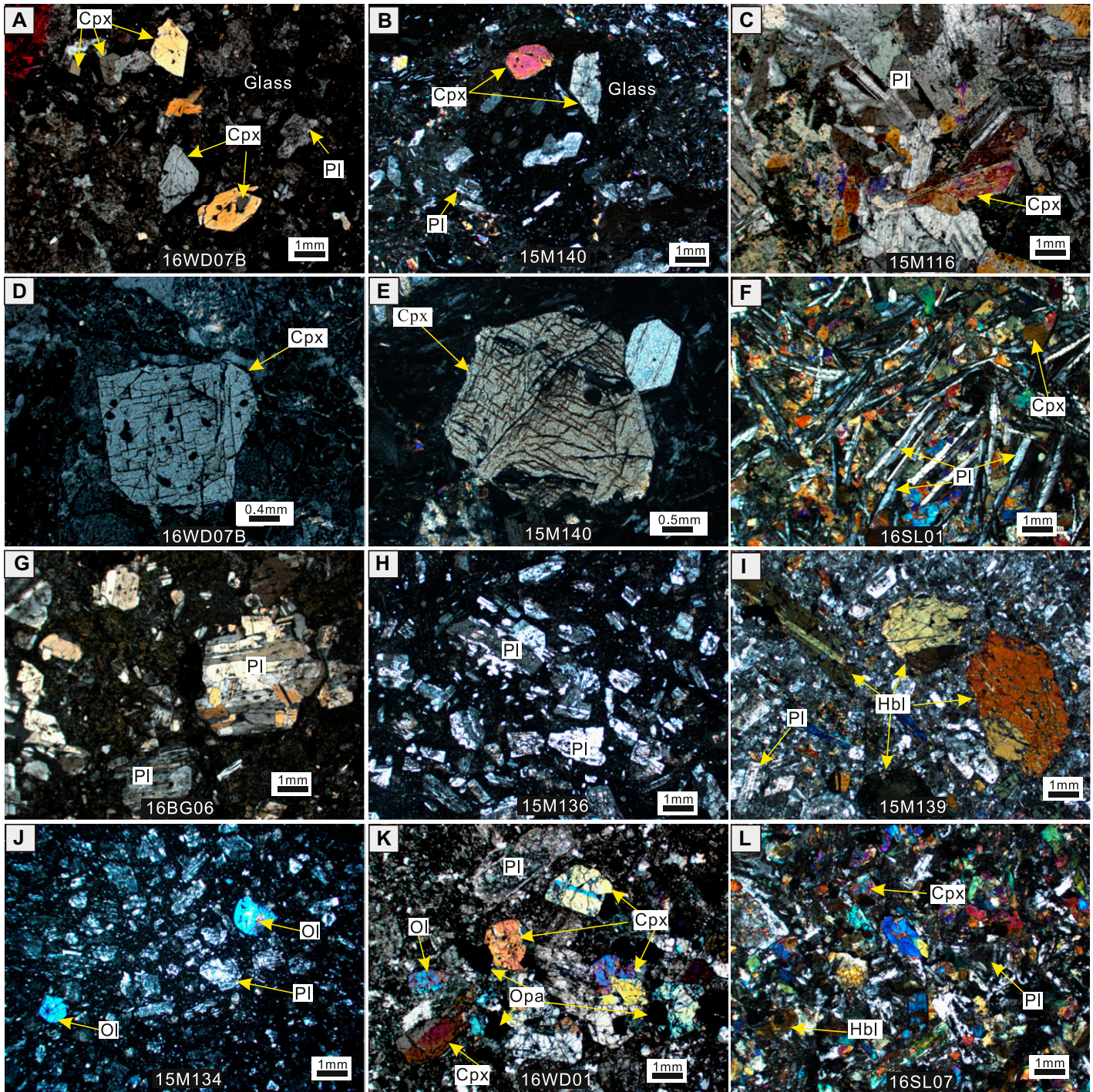


Figure 4. Cross-polarized-light photomicrographs of the mid-Cretaceous Mawgyi Volcanics in the Wuntho-Popa arc of western Myanmar. (1) Mid-oceanic ridge basalt-like rocks: Wuntho basalts with phenocrysts of abundant cpx and minor pl (A, B, D, E) and gabbro (C); (F) Salingyi dolerite with needle-like pl and cpx (F); (2) tholeiites: Wuntho basalts with pl phenocrysts and glomerocrysts (G, H) and basaltic andesites with coarse-grained hbl and pl (I); (3) calc-alkaline lavas: Wuntho basalts with ol and pl phenocrysts (J) or glomerocrysts of ol, cpx, pl, and opa (K), hbl-bearing fine-grained dolerite in Salingyi (L). ol—olivine; cpx—clinopyroxene; hbl—hornblende; pl—plagioclase; opa—opaque minerals.

in Salingyi exhibit fine-grained clinopyroxene and plagioclase with minor hornblende (Fig. 4L). The Salingyi rhyolite has some quartz phenocrysts set in the glassy matrix.

Geochronology

Zircons were obtained from crushed rocks using traditional separation techniques, and then

handpicked under a binocular microscope. Individual zircon crystals were mounted in epoxy and polished to expose the cross-sectional area of the crystals. The areas of analysis for U-Pb

dating were carefully selected through cathodoluminescent (CL) images acquired by a JSM-IT 300 scanning electron microscope located at the Institute of Tibetan Plateau Research, Chinese Academy of Sciences (ITPCAS), Beijing, China. Spots for analysis were selected to avoid inclusions and to stay within (visible) growth domains. The U-Th-Pb measurements were made using a quadrupole Agilent 7500a inductively coupled plasma-mass spectrometer (ICP-MS) coupled to a 193 nm excimer laser at ITPCAS. Each analysis contained 20 s of gas blank signal, 40 s of ablation data and 55 s of washout time. The laser energy was masked to produce a 35 μm diameter ablation pit at 7 Hz and 10 mJ/cm². Elemental and mass fractionation, and instrument drift were corrected through standard sample bracketing at a ratio 1:5 using the 91500 (1065.4 \pm 0.6 Ma, $n = 28$; Wiedenbeck et al., 2004) and Plešovice (337.1 \pm 0.4 Ma, $n = 28$; Sláma et al., 2008) zircon reference materials. The fractionation and drift corrections were made using GLITTER 4.0 and the initial-Pb corrections followed the approach of Andersen (2002). Age calculations and Concordia diagrams were produced using Isoplot software (Ludwig, 2003). Zircon U-Pb isotopic data for the Mawgyi Volcanics are presented in Supporting Information Table S2¹.

Whole-Rock Geochemistry

Samples showing minimal signs of alteration ($N = 83$) were powdered to $<74 \mu\text{m}$ for whole-rock geochemical analysis. Loss-on-ignition was measured after one hour of baking at 1000 °C. Sample powders (0.5 g) were fused with 5 g of lithium tetraborate ($\text{Li}_2\text{B}_4\text{O}_7$) at 1050 °C for 20 min and cooled as glassy flakes. Major element concentrations were then determined using an AXIOS X-ray fluorescence spectrometer at the Institute of Geology and Geophysics, Chinese Academy of Sciences, Beijing, China. Analytical uncertainties are generally better than $\pm 1\%$ for all major elements. Trace elements (including rare earth elements, REEs) were determined using aerosolized solution and a Thermo Quadrupole ICP-MS at ITPCAS. Sample powders (40 mg) were dissolved in 1 ml

of distilled 20 N HF and 0.5 ml of 7.5 N HNO_3 in capsules, then enclosed with alloy steel sleeves and heated to 170 °C for seven days. The solutions were dried and re-dissolved within 2 ml of 7.5 N HNO_3 . Finally, the solutions were diluted in 2% HNO_3 to 50 ml before analysis. BHVO-1 and BCR-1 reference materials were used to monitor the accuracy and reproducibility; standard deviation was better than $\pm 5\%$. Sr- and Nd-isotopes were measured on a Nu Plasma II multi-collector ICP-MS at ITPCAS; methodologies followed Wang et al. (2017b). Samples for Sr and Nd isotopic analysis were digested in an acid mixture of HF- HNO_3 in Teflon bombs at 150 °C for 48 h. Sr and Nd were separated in cation exchange columns containing the AG50W-X4 resin and TODGA resin, respectively. Measured $^{87}\text{Sr}/^{86}\text{Sr}$ and $^{143}\text{Nd}/^{144}\text{Nd}$ ratios were normalized to $^{146}\text{Nd}/^{144}\text{Nd} = 0.7219$ and $^{86}\text{Sr}/^{88}\text{Sr} = 0.1194$ for mass fractionation corrections. The NBS987 and JNd₁-1 international standards were used to assess instrument stability during data collection. The total procedural blanks were 70 pg for Nd and 300 pg for Sr, which were negligible considering the measured Nd-Sr concentrations of samples. During the course of this study, the mean $^{87}\text{Sr}/^{86}\text{Sr}$ value for NBS987 was 0.710239 \pm 9 ($n = 10$, 2σ) and the mean $^{143}\text{Nd}/^{144}\text{Nd}$ for JNd₁-1 was 0.512120 \pm 6 ($n = 10$, 2σ). In addition, BCR-2 yielded $^{87}\text{Sr}/^{86}\text{Sr} = 0.705006 \pm 8$ and $^{143}\text{Nd}/^{144}\text{Nd} = 0.512631 \pm 6$ ($n = 5$, 2σ). For routine analyses, the 2σ analytical errors were <0.000020 for $^{87}\text{Sr}/^{86}\text{Sr}$ and <0.000010 for $^{143}\text{Nd}/^{144}\text{Nd}$. Major and trace element data and Sr- and Nd-isotopic compositions for the Mawgyi Volcanics are presented in Supporting Information Table S3 (see footnote 1).

RESULTS

Geochronological Results

Zircons from sample 15M116 (gabbro) do not show oscillatory zoning in CL. The crystals are mostly euhedral and colorless in the range of ~ 100 – $200 \mu\text{m}$ in size with aspect ratios of 2:1–3:1. Twenty-four analyses have Th/U ratios of 0.34–0.90 and yield a Concordia $^{206}\text{Pb}/^{238}\text{U}$ age of 93.69 \pm 0.25 Ma (mean square weighted deviation [MSWD] = 1.8, $n = 24$; Fig. 5A). Zircons from sample 15M109C (basaltic andesite) are colorless and euhedral and are ~ 50 – $150 \mu\text{m}$ in length with aspect ratios from 1:1–4:1. These zircons have high Th/U ratios of 0.53–0.81 and show oscillatory zoning in CL images. Eighteen analyses on zircon crystals yield $^{206}\text{Pb}/^{238}\text{U}$ ages between 100 \pm 2 Ma and 108 \pm 2 Ma, with a Concordia age of 105.7 \pm 0.3 Ma (MSWD = 0.42,

$n = 18$; Fig. 5B). Thirteen zircons from sample 15M114A (basaltic andesite) show two subgroups in CL images. Five zircons that show a bright luminescence response and oscillatory zoning have high Th/U ratios of 0.53–1.09 and yield $^{206}\text{Pb}/^{238}\text{U}$ ages between 98 and 110 Ma with a mean age of 104 \pm 3 Ma (MSWD = 13, $n = 7$; Fig. 5C). Six other zircons with a low luminescence response have lower Th/U ratios of 0.19–0.33 and yield much older $^{206}\text{Pb}/^{238}\text{U}$ and $^{206}\text{Pb}/^{207}\text{Pb}$ ages ranging from 339 to 2229 Ma. Zircon grains from 15M139B (andesite) are colorless and euhedral are ~ 80 – $150 \mu\text{m}$ in length with aspect ratios of 1:1–3:1. Zircon grains with Th/U ratios of 0.48–0.98 yield a mean $^{206}\text{Pb}/^{238}\text{U}$ age of 93.5 \pm 2.4 Ma (MSWD = 3.3, $n = 19$; Fig. 5D) and only one grain, with high Th/U ratios (1.56) yields an older $^{206}\text{Pb}/^{207}\text{Pb}$ age of 1221 \pm 20 Ma. The zircons crystals of 16SL05A (rhyolite) are pink, and exhibit oscillatory zoning. Twenty analyses of 16SL05A zircon crystals with high Th/U ratios of 0.54–1.05 yield a Concordia age of 100.7 \pm 0.2 Ma (MSWD = 3.3, $n = 20$; Fig. 5E). Our new dating results, together with one $^{40}\text{Ar}/^{39}\text{Ar}$ age (100.9 \pm 0.2 Ma; Westerweel et al., 2019), show that the Mawgyi Volcanics formed between 105 Ma and 93 Ma. This is the oldest magmatic pulse recognized for the Wuntho-Popa arc.

Geochemical Results

The lack of easily identified marker horizons in the Mawgyi Volcanics, the lack of distinctive field characteristics in the volcanic successions, and the large spatial extent of the exposures associated with ophiolites (Mitchell, 1993) necessitate a geochemical approach to describe these rocks. Such an approach has often been applied to study the SSZ ophiolites elsewhere (e.g., Dilek and Thy, 2009). Because the Mawgyi pillow lavas and dikes show some signs of hydrothermal alteration, it is important to focus on elements that are relatively stable during such processes. In general, low-temperature reactions between seawater and rocks result in minor leaching of Fe and Si, and enrichment of Na and Mg. Alternatively, Al, P, and Ti are the least mobile elements, and Ca is usually depleted (Seyfried and Mottl, 1982). The trace elements of Cr, Co, Ni, V, high field strength elements (HFSEs: Nb, Ta, Hf, Zr, Ti, Th), REEs, and Y are relatively immobile during alteration (Pearce and Norry, 1979; Seyfried and Mottl, 1982). K, Rb, and Cs have been shown to be enriched during alteration of volcanic glass rinds in pillow basalts (Staudigel and Hart, 1983). Ba exhibits variable alteration trends (Humphris and Thompson, 1978) and Pb

¹Supplemental Material. Age information on ophiolites and arcs from Myanmar and Andaman, geochronological and geochemical data for the mid-Cretaceous Mawgyi Volcanics in the Wuntho-Popa arc of western Myanmar, and published ages associated with the Neotethyan ophiolites and island arcs, with which the reader can replicate our analyses. Please visit <https://doi.org/10.1130/GSAB.S.14720742> to access the supplemental material, and contact editing@geosociety.org with any questions.

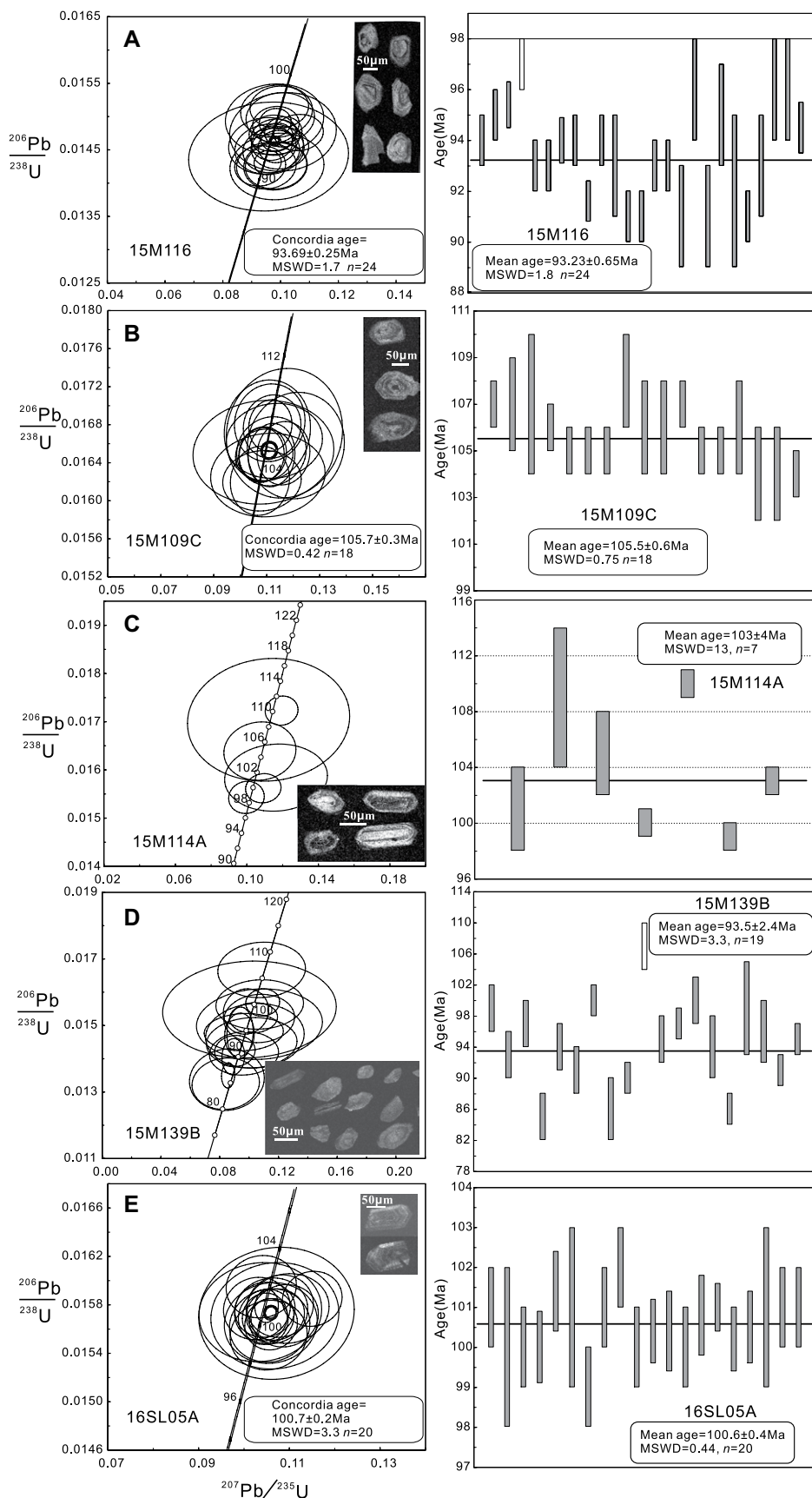


Figure 5. Zircon U-Pb ages and cathodoluminescence images of the Mawgyi Volcanics in the Wuntho-Popa arc of western Myanmar. Wuntho: (A) gabbro (15M116); (B) and (C) basaltic andesites (15M109C and 15M114A); (D) andesite (15M139B); Salingyi: (E) rhyolite (16L05A). MSWD—mean square weighted deviation.

typically becomes depleted relative to unaltered rocks (Teagle and Alt, 2004). Therefore, those elements that are resistant to hydrothermal alteration are primarily used here to build the geochemical diagrams and classify the Mawgyi Volcanics. This study focuses on the basaltic rocks, which carry the most suitable information regarding mantle melting and the tectonic settings. Herein, the geochemical data for the Salingyi rhyolite (16SL05) are provided and its origin was possibly ascribed to extremely fractional crystallization from nearby dolerites or the slab melting of the young oceanic crust (Peacock et al., 1994).

All of the rocks studied here exhibit low-K to medium-K signatures (Fig. 6A), although K_2O may have been enriched during alteration (Staudigel and Hart, 1983). Three types of rocks are identified on the basis of their distinctive REE patterns (normalized to normal (N)-MORB values; Gale et al., 2013). These include: (1) tholeiitic basalts and dolerites that exhibit flat REE patterns like MORBs with La_N of 0.3–0.8 (Fig. 6C), but lower TiO_2 (0.6–1.1 wt%; Fig. 7), and P_2O_5 (0.02–0.15 wt%). These rocks are more depleted in REEs and HFSEs (except for Th) concentrations (Figs. 7A–7J) but have higher V/Ti ratios (Fig. 8C) than those of MORBs. These geochemical signatures resemble the protoarc basalts either in the Izu-Bonin-Mariana (IBM) forearc (Ishizuka et al., 2011a; Reagan et al., 2010; Shervais et al., 2019) or at the International Ocean Discovery Program (IODP) Site U1438 (Arculus et al., 2015; Hickey-Vargas et al., 2018; Yagodziniski et al., 2018). We note that the light REE (LREE) depletions are more pronounced in the Salingyi dolerites than in the Wuntho volcanic rocks (Fig. 6C). The coarse-grained gabbro sample exhibits no positive Eu anomaly, which suggests that it is a crystallized melt instead of a cumulative dike. This gabbro sample also has a flat REE pattern and the lowest total REE concentration which is similar to the nearby volcanic rocks (Fig. 6C). (2) The island arc tholeiites show slightly fractionated REE patterns with La_N of 0.9–1.9. (3) The island arc calc-alkaline rocks are characterized by their strongly fractionated REE patterns with La_N of 2–4. All these rocks exhibit significant HFSE

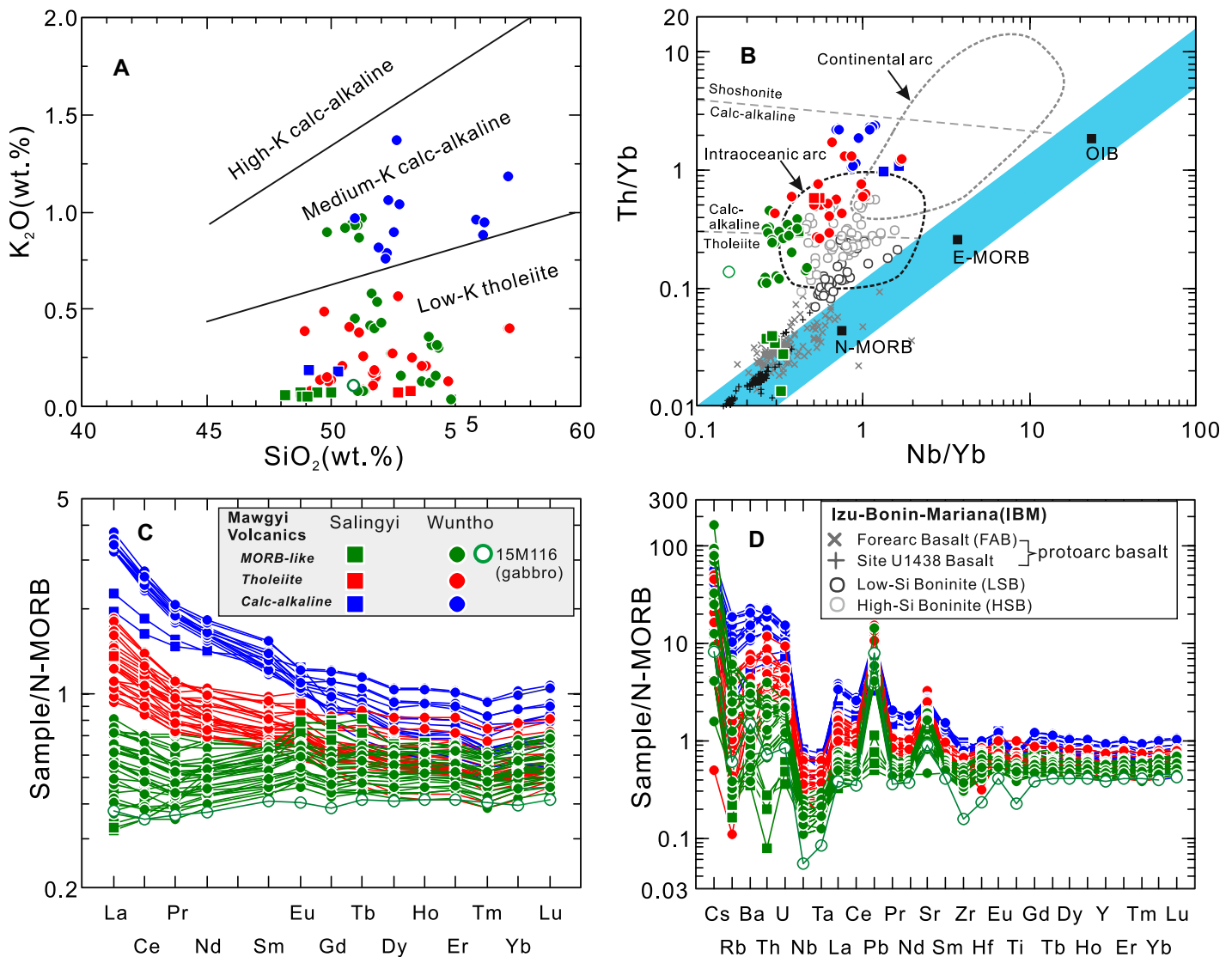


Figure 6. Geochemical classifications of the Mawgyi Volcanics in the Wuntho-Popa arc of western Myanmar. (A) K_2O versus SiO_2 (Peccherillo and Taylor, 1976); (B) Th/Yb versus Nb/Yb (Pearce, 2008); (C) Normal mid-oceanic ridge basalt (N-MORB)-normalized rare earth element patterns; (D) N-MORB-normalized multi-element diagram. The N-MORB values and Indian mid-oceanic ridge basalt (MORB) data are from Gale et al. (2013); Data of the Eocene depleted basalts and boninites in the Izu-Bonin-Mariana forearc and the International Ocean Discovery Program (IODP) Site U1438 are from the literature (Arculus et al., 2015; DeBarì et al., 1999; Haugen, 2017; Hickey-Vargas et al., 2018; Ishizuka et al., 2011a; Kanayama et al., 2012; Reagan et al., 2010, 2015; Shervais et al., 2019; Yajima and Fujimaki, 2001). The drilling IODP Site U1438 is located west of the Kyushu-Palau Ridge and within the Amami Sankaku Basin in the northwest of the Philippine Sea plate. The classification of the high-Si and low-Si boninite series follows Kanayama et al. (2013); the fields for distinguishing the intraoceanic arc from the continental arc are defined by data compiled from Schmidt and Jagoutz (2017). E-MORB—enriched MORB; OIB—ocean island basalt.

troughs and Sr, Pb spikes in the N-MORB-normalized multiple-element diagram (Fig. 6D); these signatures are indicative of arc magmas (Pearce and Peate, 1995; Schmidt and Jagoutz, 2017). There is a systematic increase of Th/Yb from the MORB-like to island arc tholeiitic and calc-alkaline rocks (Fig. 6B). Th enrichments of the MORB-like rocks are less pronounced than those of island arc tholeiite and calc-alkaline rocks, but all do show an affinity with the

intraoceanic arc rather than the continental arc (Fig. 6B; Pearce and Peate, 1995; Schmidt and Jagoutz, 2017).

Although the freshest samples were selected for isotope analysis, the effects of hydrothermal alteration cannot be completely precluded, in particular for Sr isotopes. All the rocks have $^{87}Sr/^{86}Sr_i$ ratios between 0.7041 and 0.7054, indistinguishable from those of the altered oceanic crust (AOC). The MORB-like and island

arc tholeiitic rocks exhibit relatively higher ϵNd_i values (+7 to +3) than those of island arc calc-alkaline rocks (+5.4 to +1.0), but all rocks have slightly lower ϵNd_i values than those of the modern Indian MORBs (Fig. 9A; Gale et al., 2013). The Mawgyi Volcanics are slightly more depleted in initial Nd isotope than those of the Wuntho-Popa batholiths, but are distinct from and much more juvenile than the Mogok-Mergui batholiths (Sibumasu continental arc; Fig. 9A).

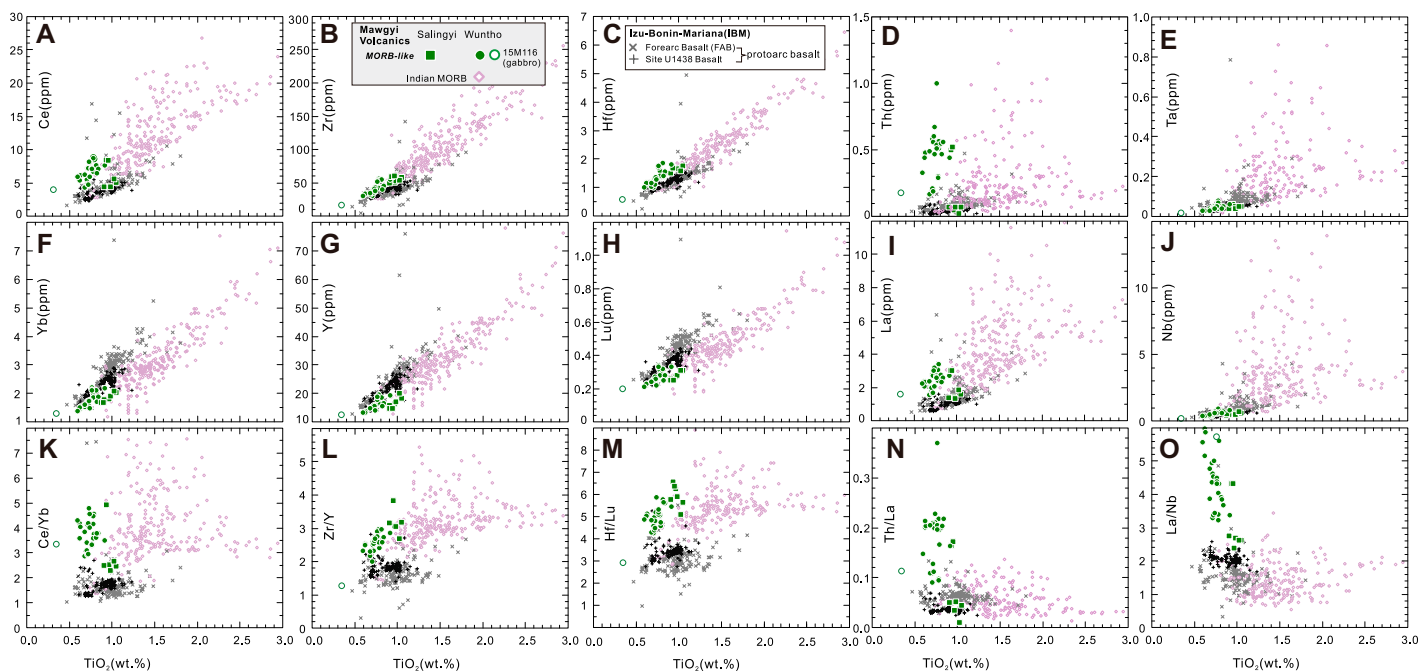


Figure 7. Selected fluid-immobile trace element abundances and ratios versus TiO_2 comparing the Mawgyi mid-oceanic ridge basalt (MORB)-like rocs from the Wuntho-Popa arc of western Myanmar with the Indian MORBs (Gale et al., 2013) and the IBM protoarc basalts. TiO_2 versus Ce (A), Zr (B), Hf (C), Th (D), Ta (E), Yb (F), Y (G), Lu (H), La (I), Nb (J), Ce/Yb (K), Zr/Y (L), Hf/Lu (M), Th/La (N), and La/Nb (O). Data sources for the IBM protoarc basalts and the Indian MORBs are the same as in Figure 6.

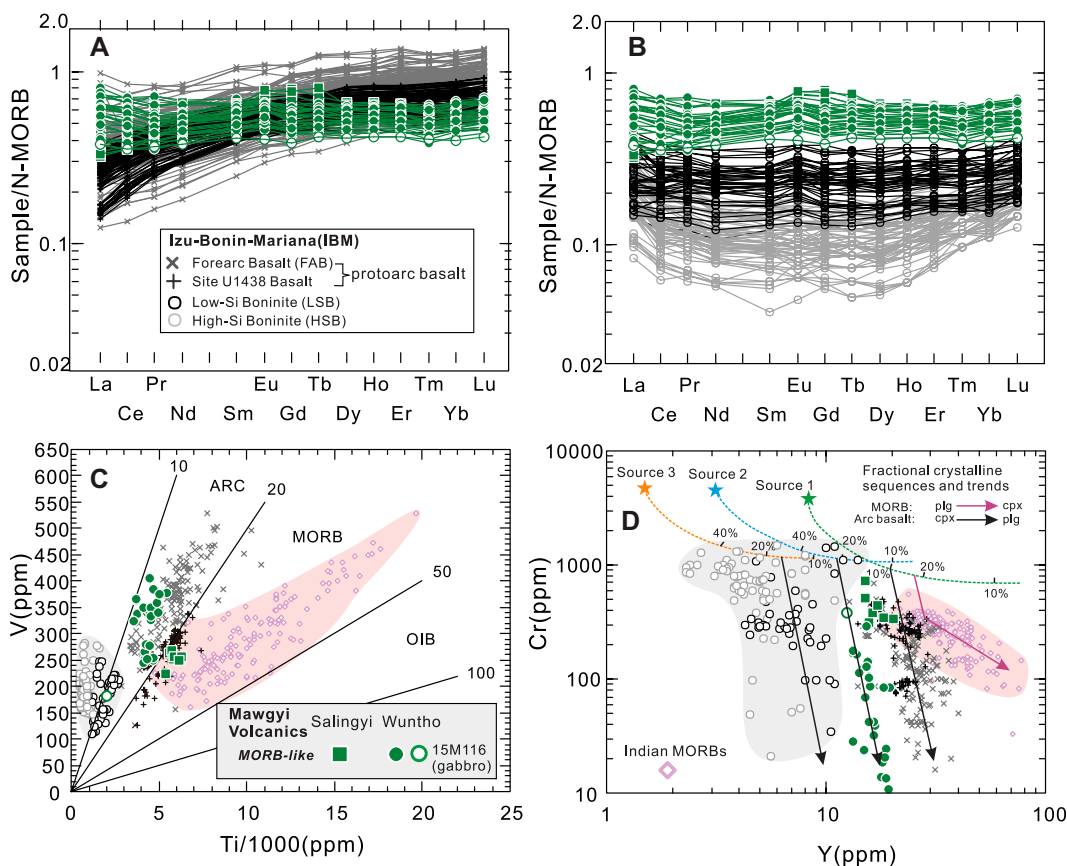


Figure 8. Rare earth element patterns of the Mawgyi mid-oceanic ridge basalt (MORB)-like rocks from western Myanmar compared with the IBM protoarc basalts (A) and boninites (B); (C) V versus Ti diagram (Shervais, 1982); (D) Cr versus Y diagram (Pearce et al., 1984). The dashed curves represent incremental batch melting trends and sources 1, 2, and 3 represent source compositions from Murton (1989) and Pearce et al. (1984). Mantle Source 1 represents a calculated plagioclase (plg) lherzolite containing 0.60 olivine + 0.20 orthopyroxene + 0.10 clinopyroxene (cpx) and Source 2 represents the residual mantle subsequent to 20% melt (MORB) extraction from Source 1. Source 3 represents a more depleted source after ~12% extraction of Source 2. Data sources for the IBM protoarc basalts and boninites are the same as in Figure 6.

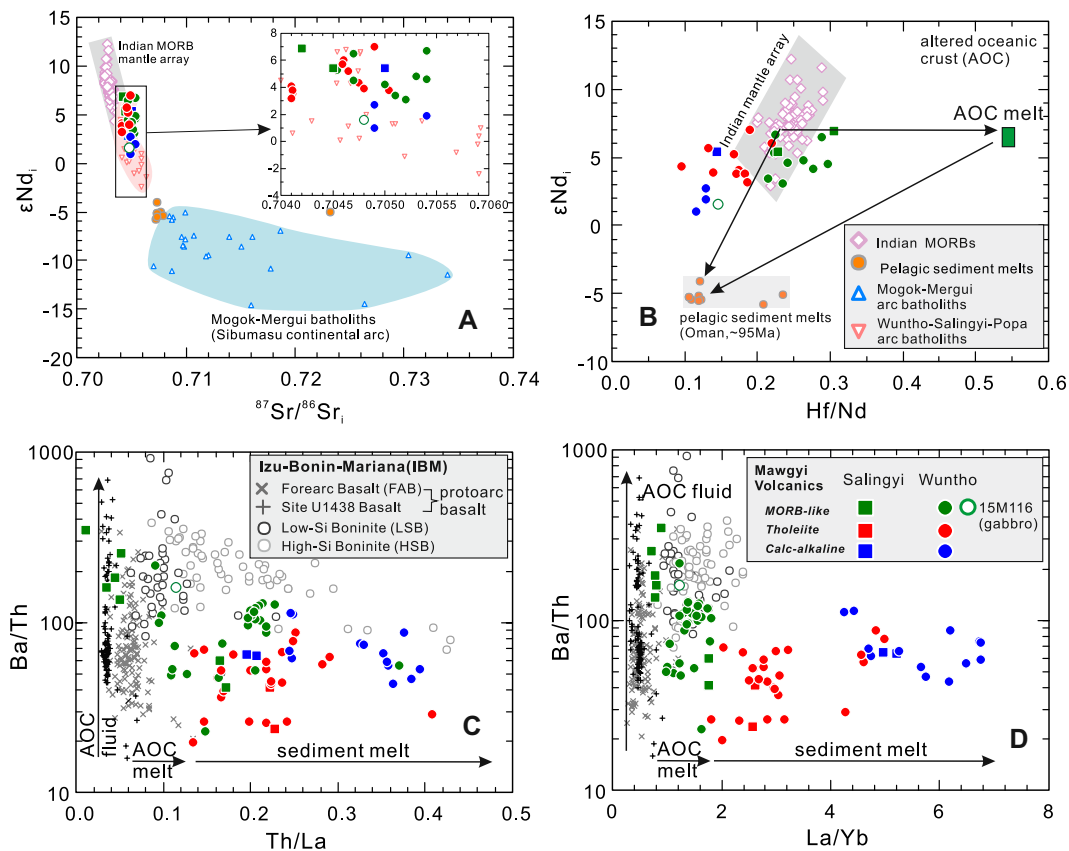


Figure 9. Geochemical characteristics of the Mawgyi Volcanics in the Wuntho-Popa arc of western Myanmar. (A) $^{87}\text{Sr}/^{86}\text{Sr}_i$ versus ϵNd_i ; (B) Hf/Nd versus ϵNd_i ; (C) Th/La; and (D) La/Yb versus Ba/Th. The Sr-Nd isotopic data for the Mogok-Mergui and Wuntho-Popa batholiths are from Li et al. (2019a, 2020a) and references therein. Geochemical data of pelagic sediment-derived melts (ca. 95 Ma) in Oman ophiolites are from Haase et al. (2015). The amphibolite-facies melt of altered oceanic crust (AOC) is assumed to have Hf/Nd of ~ 5.5 (Li et al., 2019b). Data sources for the IBM protoarc basalts and boninites are same as in Figure 6. MORB—mid-oceanic ridge basalt.

DISCUSSION

Origin of the Mawgyi Volcanics

Investigations of the modern Izu-Bonin-Mariana (IBM) forearc system led to the conclusion that the sequences of distinctive magmatic types generated during subduction initiation are layers of tholeiitic basalts, followed by, and to some extent concurrent with, boninites, and then succeeded by more typical island arc tholeiite and calc-alkaline rocks (DeBari et al., 1999; Ishizuka et al., 2011a, 2011b; Pearce et al., 1992; Reagan et al., 2010, 2019; Stern and Bloomer, 1992). The IBM earlier tholeiitic basalts are more depleted in lithophile trace elements than MORBs but less depleted than boninites. Reagan et al. (2010) termed these depleted basalts as forearc basalts (FABs) and described them as tholeiites with trace element patterns more depleted than average MORBs (Figs. 7A–7J) but lacking subduction components (Figs. 9C and 9D). These depleted magmas were interpreted as the initial products of decompression melting by upwelling asthenosphere above the leading edge of a newly foundering oceanic plate during subduction initiation (e.g., Reagan et al., 2010, 2015; Shervais et al., 2019). Boninites, nearly simultaneous with FABs (Reagan et al., 2019), exhibit

chemical signals of subduction influence as they were extremely depleted in TiO_2 ($<0.5\%$) and heavy REEs (Fig. 8B; Pearce et al., 1992; Umino et al., 2015), and were probably generated by fluid-flux mantle remelting of the FAB residues at relatively lower potential melting temperatures (e.g., Langmuir et al., 2006; Lee et al., 2009). Alternatively, the basaltic basalts from the IODP Site U1438 are indistinguishable from the IBM FABs with respect to trace elements and isotopes (Arculus et al., 2015; Hickey-Vargas et al., 2018; Yogodzinski et al., 2018; Locus of data in fig. 1 of Arculus et al., 2015), but boninites have not been recognized in this location yet. Prior to drilling by the IODP Expedition 351, the basaltic section at IODP Site U1438 was inferred to be the pre-existing Cretaceous oceanic crust where the IBM arc was built (e.g., Ishizuka et al., 2011b). However, recent findings indicate that the IODP Site U1438 basalts may have formed within the earliest 3 Ma of subduction initiation in a region close to but farther from the Pacific plate edge than boninites (Arculus et al., 2015; Ishizuka et al., 2018; Hickey-Vargas et al., 2018; Yogodzinski et al., 2018). Collectively, the depleted basalts and boninites in the modern IBM forearc and in the IODP Site U1438 represent the protoarc crust above a near-trench seafloor spreading center during

a period immediately following subduction initiation (ca. 52 Ma, Arculus et al., 2015; Hickey-Vargas et al., 2018; Ishizuka et al., 2018; Li et al., 2019a; Reagan et al., 2015, 2019; Shervais et al., 2019; Yogodzinski et al., 2018). In this context, our geochemical results indicate that the Mawgyi Volcanics are dominated by the MORB-like rocks, which resemble the IBM protoarc basalts. It is generally thought that the Indian asthenospheric mantle prevailed during the Eocene IBM subduction initiation (e.g., Hickey-Vargas, 1998; Li et al., 2019a; Yogodzinski et al., 2018) and that the Neotethyan Ocean was also governed by the Indian Ocean mantle domain (e.g., Mahoney et al., 1998; Zhang et al., 2005). Thus, a complete comparison to the IBM protoarc basalts and to the modern Indian MORBs (Gale et al., 2013) is performed below to better understand the origin of the Mawgyi MORB-like rocks (Figs. 6–8).

The Mawgyi MORB-like rocks exhibit flat REE patterns (Fig. 6C) but are characterized by depletions in REEs, HSFs (except for Th), and TiO_2 abundances when compared with the Indian MORBs, which resembles those of the IBM protoarc basalts (Fig. 7). However, some minor differences between the Mawgyi MORB-like rocks and the IBM protoarc basalts are also illustrated below. For example, the Mawgyi MORB-like rocks show flatter REE

patterns relative to those of the IBM protoarc basalts (Fig. 8A). The Mawgyi MORB-like rocks are systematically more enriched in Ce, Zr, and Hf (Figs. 7A–7C) but depleted in Yb, Lu, and Y (Figs. 7F–7H), resulting in the higher ratios of Ce/Y, Zr/Y, and Hf/Lu than those of the IBM protoarc basalts (Figs. 7K–7M). Th enrichments are more significant for the Mawgyi MORB-like rocks than for the IBM protoarc basalts (Fig. 7D). Particularly, the Wuntho volcanic rocks carry a unique sediment-enrichment signature with high Th/La ratios (Plank, 2005; Fig. 7N). Similar sediment-enrichment signatures have not been recognized in the Salingyi dolerites or in the IBM protoarc basalts (Li et al., 2019a; Shervais et al., 2019; Yagodinski et al., 2018). Additionally, the Wuntho volcanic rocks are more enriched in LREEs than those of the Salingyi dolerites, resulting in higher La/Nb of typical arc signatures (Fig. 7O). In comparison with the IBM forearc boninites, the Mawgyi MORB-like rocks have flat REE patterns akin to the low-Si boninites, but are more enriched in total REEs (Fig. 8B).

The diagnostic Ti–V diagram of Shervais (1982) clearly shows that the Mawgyi MORB-like rocks are similar to those of the IBM protoarc basalts but differ from the Indian MORBs (Fig. 8C). Two causal mechanisms for this distinctive geochemical signature can be used to distinguish the IBM FABs from MORBs: mantle source depletion in Ti and enrichment in V during melting at a more oxidizing state (Reagan et al., 2010). The first scenario suggests that Ti depletion in FABs relative to MORBs can either have resulted from higher degrees of partial melting of fertile mantle or inherited, in part, from a more depleted mantle source (Shervais et al., 2019). Thermodynamic calculations and experimental results indicated that mantle melting through fluid fluxing will be enhanced and resulted in higher degrees of melting (Grove et al., 2006; Hirschmann et al., 1998), thus leading to depletion of Ti in the IBM FABs relative to the MORBs. The relative degrees of partial melting can be estimated by using the Cr–Y diagram (e.g., Murton, 1989; Pearce et al., 1984). The Mawgyi MORB-like rocks exhibit higher degrees of partial melting than those of IBM protoarc basalts but lower than those of the IBM forearc boninites (Fig. 8D). Such uniquely depleted basalts can be expected as a reflection of the distinctive mantle melting during subduction initiation. Mantle depletion events also have been linked to higher degrees of partial melting under more oxidizing conditions during subduction initiation (Reagan et al., 2010). The second scenario invokes the reasoning of Shervais (1982) where the island arc basalts have lower Ti/V ratios

relative to MORBs because mantle source oxidations dramatically increase even with a small amount of fluid fluxing. These oxidizing conditions of the mantle may be established quickly when the slab dehydration commences during subduction initiation beneath a hot and incipient asthenospheric wedge (e.g., Brounce et al., 2015). In this context, the Salingyi dolerites were produced under less oxidizing conditions than those of the Wuntho volcanic rocks. Crucially, the Wuntho volcanic rocks are more akin to the IBM FABs, whereas the Salingyi dolerites would be more closely related to the IODP Site U1438 basalts (Fig. 8C). As such, the Wuntho volcanic rocks were erupted above the incipient slab while the Salingyi dolerites were intruded at a distance from the slab edge.

Definitive identification for subduction enrichment of the IBM protoarc basalts is difficult to assess with whole-rock geochemical data because enrichment of these fluid-mobile elements (e.g., U, K, Rb, Sr, Pb, Ba) could be either an igneous signature of primary magmas sourced from slab-derived hydrous fluids, or could be introduced from seawater alteration (e.g., Hickey-Vargas et al., 2018), or both. The least-altered glasses in a majority of IBM FABs lack geochemical evidence for involvement of slab-derived hydrous fluids (Coulthard et al., 2017). In addition, Th depletion and low Th/La ratios preclude sediment melts to form the IBM FABs (Fig. 9C). New measurements of radiogenic isotopes support the previous conclusion again that the IBM FABs do not have discernible subduction-related components (Li et al., 2019a). Surprisingly, the coeval forearc boninites carry the geochemical signatures of significant slab contributions including the presence of hydrous fluids, sediment-derived melts, and even melts from altered oceanic crust (Coulthard et al., 2017; Li et al., 2019a; Pearce et al., 1992; Reagan et al., 2019). La is fluid-mobile but more resistant to alteration than Ba. The La/Yb of the Mawgyi MORB-like rocks are consistently higher than those of IBM protoarc basalts (Fig. 9D). This suggests some slab-derived fluids contributed to the production of the Mawgyi MORB-like rocks. In particular, the Salingyi dolerites and the IBM protoarc basalts are indistinguishable with respect to Th, Th/Yb, Th/Nb, and Th/La (Figs. 7D, 6B, 9C, and 9D). This means that the Salingyi dolerites lack traditional compositional signals of subduction enrichment. The Wuntho volcanic rocks are significantly enriched in Th and thus much higher Th/Nb and Th/La than those of IBM protoarc basalts (Figs. 7D, 6B, and 9C). Crucially, this suggests that the Wuntho volcanic rocks carry a prominent signal of slab-derived melts. In general, Th/La is a use-

ful tracer of sediment recycling at subduction zones (Plank, 2005). The Th/La is pronounced in the Wuntho volcanic rocks, indicating additions of sediment-derived melts (Fig. 9C). The initial Nd isotopic values of the Mawgyi MORB-like rocks are lower than those of the Indian MORBs data (Fig. 9A), if the sediment-derived melts had initial Nd isotopic values like those found in Oman ophiolites (ca. 95 Ma; Haase et al., 2015; Fig. 9B). Furthermore, Hf/Nd and initial Nd isotopic values can be used to distinguish a sediment-melt from an AOC melt; AOC melts are characterized by higher Hf/Nd ratios (~0.55; Li et al., 2019a). The Mawgyi MORB-like rocks have slightly higher Hf/Nd ratios than those of the Indian MORBs, suggesting input of AOC melts (Fig. 9B). We propose that AOC melts, such as the Salingyi rhyolites with low Sr/Y ratios (~8), were probably generated at shallow depths and hot environments as a result of high-temperature amphibolitic and/or granulitic melting (Green et al., 2016; Soret et al., 2017).

The geochemical signatures of the Mawgyi tholeiite and calc-alkaline rocks with moderately to highly fractionated REE patterns (Fig. 6C) suggest little input of AOC melts (Fig. 9B) but some involvement of subducted sediments (Figs. 6B, 9C, and 9D). The Mawgyi tholeiite and calc-alkaline rocks are distinct with respect to Th/Yb (Fig. 6B), Th/La (Fig. 9C), and La/Yb (Fig. 9D). The relative depletions and enrichments in trace element denote the intraoceanic arc magmas globally (Figs. 6B and 6D; Schmidt and Jagoutz, 2017; Stern, 2002).

A Continental or an Intraoceanic Arc?

It has been proposed that the Early Cretaceous Western Belt ophiolites within the Indo-Burma ranges were connected to the Yarlung-Tsangpo ophiolites (Fareeduddin and Dilek, 2015; Htay, 2017; Liu et al., 2016a; Niu et al., 2017), which may have formed in a continental forearc setting at a pre-existing subduction zone (e.g., Dai et al., 2013; Maffione et al., 2015a; Qian et al., 2020). Sediments sourced from the Lhasa terrane—the southernmost of the Gondwana derived Tibetan terranes—were deposited on these ophiolites (Laskowski et al., 2019; Orme et al., 2015; Wang et al., 2017a) and filled the Xigaze forearc basin at ~16.5°N paleolatitude (Huang et al., 2015). The Kanza Chaung Batholith and Kondan Chaung Group in the Wuntho ranges are the northern segments of the Wuntho-Popa arc (Fig. 3A). New paleomagnetic constraints yielded a southern hemisphere paleolatitude of ~5°S between 97 Ma and 87 Ma (Westerweel et al., 2019). If the Wuntho-Popa arc was the southeastern con-

tinuation of the Gangdese arc (Li et al., 2020a; Lin et al., 2019; Wang et al., 2014; Zhang et al., 2017b; Zhang et al., 2018), it necessitates the configuration along the southernmost Asian continental margin to be orientated nearly N-S between 97 Ma and 87 Ma. That scenario would have resulted in a hyper-oblique subduction zone unfavorable to explain the extensive arc magmatism in Myanmar (Fig. 2). These paleomagnetic results thus have two major tectonic implications (Westerweel et al., 2019): (1) the Wuntho-Popa arc was separated from the Western Belt ophiolites during the mid-Cretaceous time by 20° of latitude, although presently close in latitudinal positions (Fig. 1); and (2) the mid-Cretaceous Wuntho-Popa arc was an island arc, part of the trans-Neotethyan intraoceanic arcs at a near-equatorial latitude and isolated from a continental setting from the mid-Cretaceous to the mid-Eocene. This long-period of isolation from terrigenous sediment sources potentially explains why the detritus that infilled the Central Myanmar Basin was predominantly derived from a juvenile arc, the Wuntho-Popa arc (Cai et al., 2019; Licht et al., 2018; Wang et al., 2014). There was an abrupt increase in the contribution of ancient crustal material after the mid-Eocene as the WBT moved toward the Sibumasu Terrane and the eastern Himalayan syntaxis (Licht et al., 2018; Wang et al., 2014; Westerweel et al., 2020). Crucially, the numerous Burmese amber fossils, collected from the Hukawng valley in the northern WBT (Fig. 2A) and considered to be mid-Cretaceous in age (Shi et al., 2012), provide no evidence of a Laurasian distribution at that time (e.g., Poinar, 2018). Until the mid-Eocene, the WBT was at a crossroads for plant dispersal between Gondwana and Laurasia (e.g., Huang et al., 2021). Along the lines of Westerweel et al. (2019), we speculate that the younger Andaman ophiolites, instead of the Western Belt ophiolites, would correlate with the Wuntho-Popa arc because of the large-magnitude northward translation of the WBT since mid-Eocene time along the Sagaing Fault. Displacement along the Sagaing Fault is thought to be in the range of 1100–2000 km according to the mid-Eocene paleolatitude and geologic evidence (Mitchell, 1993; Westerweel et al., 2019). Compositional similarities between the definitive Mawgyi MORB-like magmas and the IBM protoarc basalts, the temporal coincidence between the Wuntho-Popa arc and many Neotethyan ophiolites or island arcs along the eastern Mediterranean, Middle East, Pakistan, and Southeast Asia encourage us to conclude that the formation of the Mawgyi Volcanics resulted from intraoceanic subduction initiation within the Neotethys.

Spontaneous or Induced Subduction Initiation within the Neotethys?

The mechanisms and processes of intra-oceanic subduction initiation remain widely debated. These uncertainties include where subduction zones begin and how magmas respond. Two main conceptual end-member mechanisms are considered: spontaneous subduction initiation (SSI) and induced subduction initiation (ISI; Stern, 2004). SSI alone cannot explain the occurrences of the mid-Cretaceous intraoceanic arcs and SSZ ophiolites over a distance of 8000 km within the entire Neotethyan Ocean (Fig. 12). One fundamental criterion that would discern between SSI and ISI (Fig. 10) is the time lag between lower plate burial and upper plate extension (e.g., Guilmette et al., 2018). The initial burial of the lower plate is best recorded in metamorphic soles which many SSZ ophiolites rest on (e.g., Wakabayashi and Dilek, 2000). Metamorphic soles were generally derived from the uppermost crust of the subducting lower plate and preserved from further subduction by welding to the mantle section of the upper plate during subduction zone infancy, and thus have directly recorded the initial burial of the lower plate after nucleation of a subduction interface (Agard et al., 2016; Guilmette et al., 2018; Soret et al., 2017). Amphibolites exposed at the top of many metamorphic soles exhibit peak metamorphic conditions of high-temperature amphibolite and/or granulite facies (11–13 kba and ~850 °C; Agard et al., 2016; Soret et al., 2017). Metamorphism of oceanic crust in such conditions requires subduction along an anomalously hot geothermal gradient that would typically be restricted to the earliest stage of plate subduction (Agard et al., 2016; Soret et al., 2017; Wakabayashi and Dilek, 2000). Upper plate extension immediately corresponds with the lower plate sinking, resulting in upwelling of the hot asthenosphere, near-trench spreading, and formation of the IBM protoarc basalts (Hall et al., 2003; Shervais, 2001; Stern and Bloomer, 1992; Arculus et al., 2015; Hickey-Vargas et al., 2018; Ishizuka et al., 2011a, 2018; Reagan et al., 2010, 2015; Li et al., 2020b; Yogodzinski et al., 2018). In the above context, the formation of the metamorphic soles associated with the Andaman ophiolites (106–105 Ma; Plunder et al., 2020) occurred immediately prior to the onset of the Mawgyi Volcanics magmatism (105–93 Ma). Additionally, these metamorphic soles in the Andaman Islands formed much earlier than those felsic rocks (diorites, trondhjemites, and plagiogranites) associated with the ophiolites (95–93 Ma; Pedersen et al., 2010; Sarma et al., 2010). We propose that ISI provides the most likely explanation for the Wuntho-Popa

arc, especially given consideration of the spatial association between the Andaman ophiolites and the Wuntho-Popa arc during the mid-Cretaceous.

Where Did Intraoceanic Subduction Initiation Begin?

Induced subduction initiation requires special geodynamic circumstances in the ocean. For example, the nucleation of subduction along pre-existing weak zones requires far afield plate forces (Fig. 10; Stern and Gerya, 2018). The most widely distributed pre-existing weak zones within oceanic basins are transform faults (Casey and Dewey, 1984; Forsyth and Uyeda, 1975) and fracture zones (Mueller and Phillips, 1991; Toth and Gurnis, 1998). Subduction can also nucleate parallel to (ultra)slow-spreading mid-oceanic ridges (Agard et al., 2007; Gurnis et al., 2004; Maffione et al., 2015b; van Hinsbergen et al., 2015) where nearby extensional detachment faults cutting oceanic crust and deep into the mantle have been widely documented (e.g., Escartín et al., 2008; MacLeod et al., 2002; Smith et al., 2006). Ridge inversion has been proposed for subduction nucleation based on geological records within the Neotethyan Ocean and in the western Philippines (Hacker et al., 1991; Keenan et al., 2016; Maffione et al., 2015b, 2017; Nicolas and Boudier, 2017; van Hinsbergen et al., 2015). Since mid-oceanic ridges are commonly segmented by transform faults, both ridges and transform faults are likely to contribute to subduction nucleation in some form when the convergent forces oblique to the spreading direction are applied (Maffione et al., 2015b). Although it is difficult to identify exactly where subduction initiation nucleated within the Neotethyan Ocean, the E-W spatial distribution of mid-Cretaceous SSZ ophiolites and intraoceanic arcs may provide clues to discriminate between transform faults and mid-oceanic ridges (Fig. 12). If reconstructions of the Neotethyan Ocean with near E-W-trending spreading ridges are correct (Gibbons et al., 2015; Jagoutz et al., 2015; Müller et al., 2019; Seton et al., 2012; van Hinsbergen et al., 2016, 2020; Zahirovic et al., 2016), we infer that subduction initiation by large-scale ridge inversion (Fig. 11) may have been widespread within the Neotethyan Ocean during the mid-Cretaceous time (Fig. 12C).

Although the thin lithosphere adjacent to ridges could potentially be more easily deformed than cold, thick oceanic lithosphere, the negative buoyancy of young oceanic lithosphere driven by asthenospheric upwelling implies some resistance of downwarping and shearing to nucleate subduction (Cloos, 1993). However, numerical modeling experiments suggest that the resistance of young thin oceanic lithosphere to downwarp-

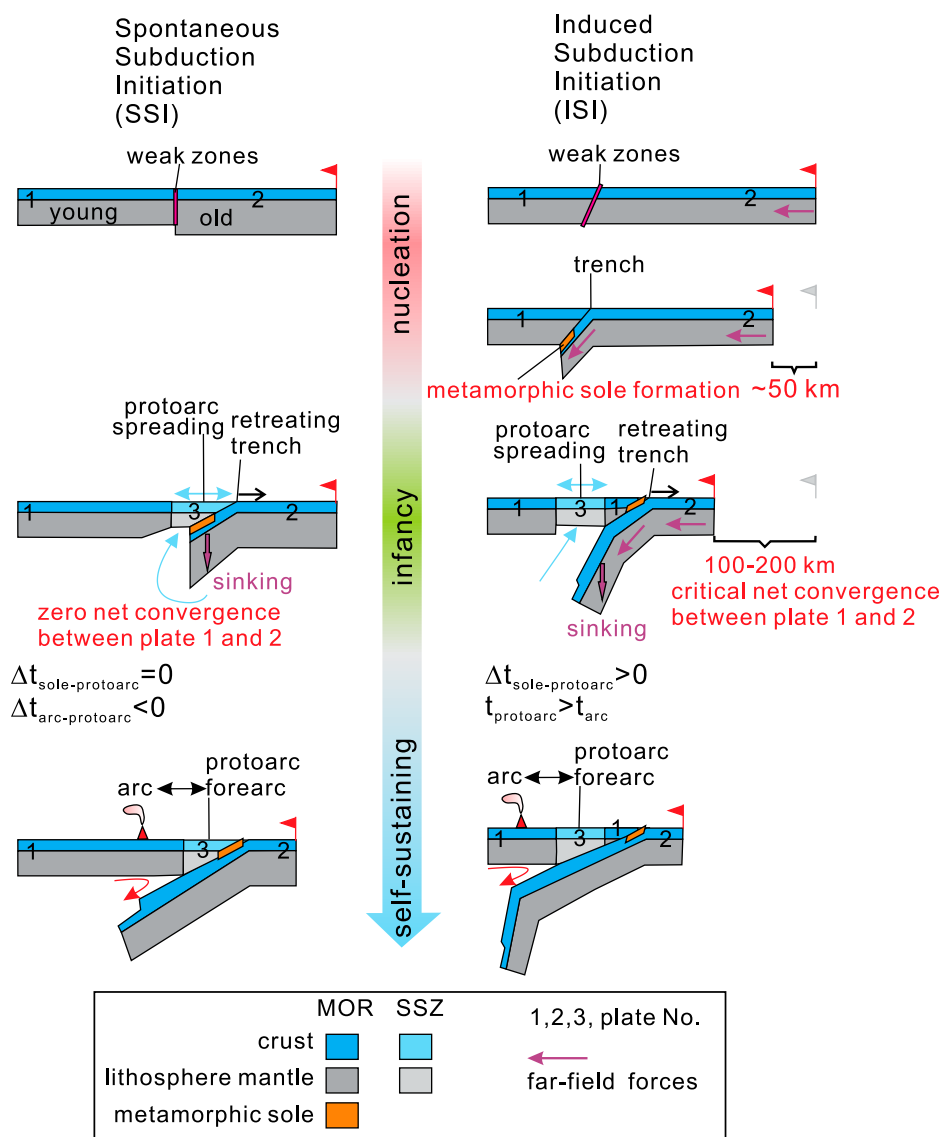


Figure 10. Conceptual models distinguishing between spontaneous and induced subduction initiation within ocean modified after Stern (2004) and Guilmette et al. (2018). One fundamental criterion that would discern between SSI and ISI is the time lag between lower plate (No. 2) burial and upper plate (No. 3) extension. Herein, we emphasize that the time lag during subduction initiation is, in fact, a function of a critical plate convergence. SSI (e.g., gravitational failure) results in a time lag of zero with zero net plate convergence. Alternatively, ISI requires a period of far afield forced convergence and results in a time lag of several million years for plate consumption. Numerical models suggest that this critical net convergence between 100 km and 200 km is least required for ISI (Gurnis et al., 2004; Hall et al., 2003; Leng and Gurnis, 2011; McKenzie, 1977), which is 2–4 times, in length, more than is necessary for metamorphic sole formation (<50 km, given initial slab dip angles between 45° and 90°; Agard et al., 2016; Soret et al., 2017). MOR—mid-oceanic ridge basalt; SSZ—supra-subduction zone.

ing and shearing may be overcome by inversion of deep-cutting detachment faults (e.g., Maffione et al., 2015b, 2017; van Hinsbergen et al., 2015) or the ridge swelling (e.g., Beaussier et al., 2019; Gülcher et al., 2019) when ridge-perpendicular compressional forces are applied. Underthrust-

ing does not localize at the spreading ridge axis, but instead at one of the pre-existing detachment faults near the spreading ridge (Fig. 11A). If valid, this suggests that the paleo-mid-oceanic ridges may be preserved in ophiolitic upper plate and that magmatism along the ridge may

continue after subduction initiation. As the leading edge of the young oceanic slab reaches a depth of 25–35 km (Fig. 11B), metamorphic soles form but self-sustaining subduction is not yet achieved until the slab reaches a depth of at least 50–150 km (e.g., Gurnis et al., 2004; McKenzie, 1977), which is shallower than or close to mantle melting depths (80–110 km) in modern subduction zones (Syracuse and Abers, 2006). This means that a shallow and hot mantle wedge would form between the upper thin plate of paleo-ridges and the lower burial plate of the young incipient oceanic slab (Fig. 11C), and be distinct from the cooler and deeper mantle wedge which characterizes most active mature subduction zones (Syracuse et al., 2010; Fig. 11C, like M3). Fluids release from slabs more efficiently at shallower depths (Iwamori, 1998). To that end, fluids-flux melting of depleted mantle after MORB extraction (Fig. 11C; M1) would produce magmas like the Mawgyi MORB-like rocks. Melting the subducted, young, and altered oceanic crust may also be expected due to the large thermal contrast between the upwelling mantle and incipient slab and also produce felsic melts like the Salingyi rhyolites. The higher Hf/Nd ratios of the Mawgyi MORB-like rocks represent input of the AOC melts, hence advocating a high geothermal gradient (Fig. 9B). However, this “hot” subduction zone, adjacent to the ridge crest, would thus be shallower and hence the felsic magmas would be characterized in composition by high-temperature amphibolitic and/or granulitic melts (tonalite, trondhjemite, and granite with low Sr/Y < 40; Salingyi rhyolites with Sr/Y ratios of ~8) instead of eclogitic melts (adakite with high Sr/Y > 40; Green et al., 2016; Peacock et al., 1994; Soret et al., 2017; Zhang et al., 2014).

The time lag between lower plate burial and upper plate extension (or between metamorphic soles and MORB-like magmas) for ISI is, in fact, a function of a critical plate convergence (Fig. 10). Gravitational failure across oceanic transform faults or fracture zones has been proposed to trigger lithosphere sinking (Maunder et al., 2020; Stern and Bloomer, 1992; Stern, 2004), resulting in a time lag of zero for net plate convergence during SSI. Alternatively, ISI requires a period of forced convergence—presumably accommodated at pre-existing weak zones—resulting in a time lag of several million years for plate consumption (Gurnis et al., 2004; Hall et al., 2003; McKenzie, 1977). In general, metamorphic soles record depths of 25–35 km from the initial lower plate burial (Agard et al., 2016; Soret et al., 2017), thus yielding a net plate convergence of no more than 50 km given initial slab dip angles between 45° and 90°. Numerical and theoretical models

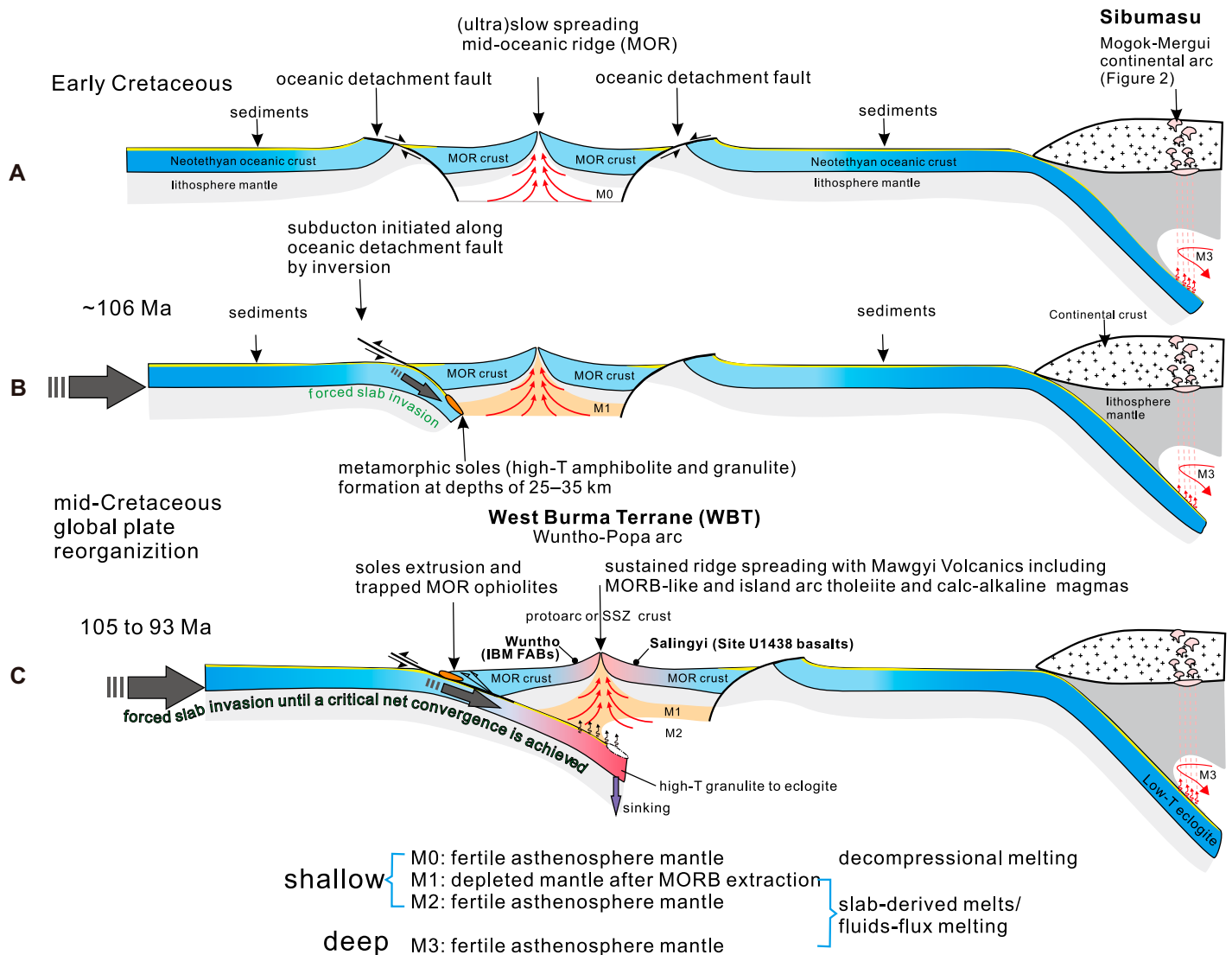


Figure 11. The conceptual model of ridge inversion for the mid-Cretaceous Neotethyan Ocean (after Kusano et al., 2017; van Hinsbergen et al., 2015). (A) Single subduction zone along the Sibumasu continental margin; (B) inversion of a detachment fault near mid-oceanic ridge driven by far-field forces and formation of the metamorphic soles; and (C) building the Wuntho-Popa protoarc after soles formation based primarily on the origin of the Mawgyi Volcanics. The Mawgyi mid-oceanic ridge basalt (MORB)-like rocks were generated by partial melting of the depleted mantle (M1; the MORB residue) and this mantle melting was enhanced by hydrous fluids, sediment, and altered oceanic crust melts which were released by the slab under high geothermal gradient. Unlike the Wuntho volcanic rocks above the slab, the Salingyi dolerites formed under less oxidizing conditions and were posited farther from the slab edge. The Mawgyi island arc tholeiite and calc-alkaline rocks were produced by wet melting of fertile and fresh asthenospheric mantle (M2) with input of hydrous fluids and sediment-derived melts at shallow depths. As the hot, young, and buoyant slab suppressed convection of this shallow mantle wedge, this infant mantle wedge ultimately cooled down, but led to subsequent mature and normal arc magmatism sourced from a deep mantle wedge (like M3). Double subduction zones between India and Asia developed within the Neotethyan Ocean after ca. 93 Ma, which better accounts for the very rapid northward drift of Indian continent during the Late Cretaceous (Fig. 3B; Gibbons et al., 2015; Jagoutz et al., 2015; van Hinsbergen et al., 2011). Between the Late Cretaceous and mid-Eocene, the significant clockwise rotation of $\sim 60^\circ$ with respect to the stable Eurasia (Westerweel et al., 2019) made the Wuntho-Salingyi-Popa intraoceanic arc parallel to the Mogok-Mergui continental arc. SSZ—supra-subduction zone; IBM FABs—Izu-Bonin-Mariana forearc basalts.

suggest that to make ISI proceed a critical net convergence of at least 100–200 km is required (Gurnis et al., 2004; Hall et al., 2003; Leng and Gurnis, 2011; McKenzie, 1977), which is 2–4 times, in length, more than is necessary

for metamorphic sole formation. The continuous subducting slab may penetrate into fertile asthenosphere immediately under a thin upper plate in a manner of ridge inversion, resulting in a mantle wedge at shallower depths and thus

arc magmatism accompanying ridge spreading (Fig. 11C). This inference is supported by the observations in the Puysegur infant subduction zone between the Indian-Australian and Pacific plates. Highly oblique convergence in the past

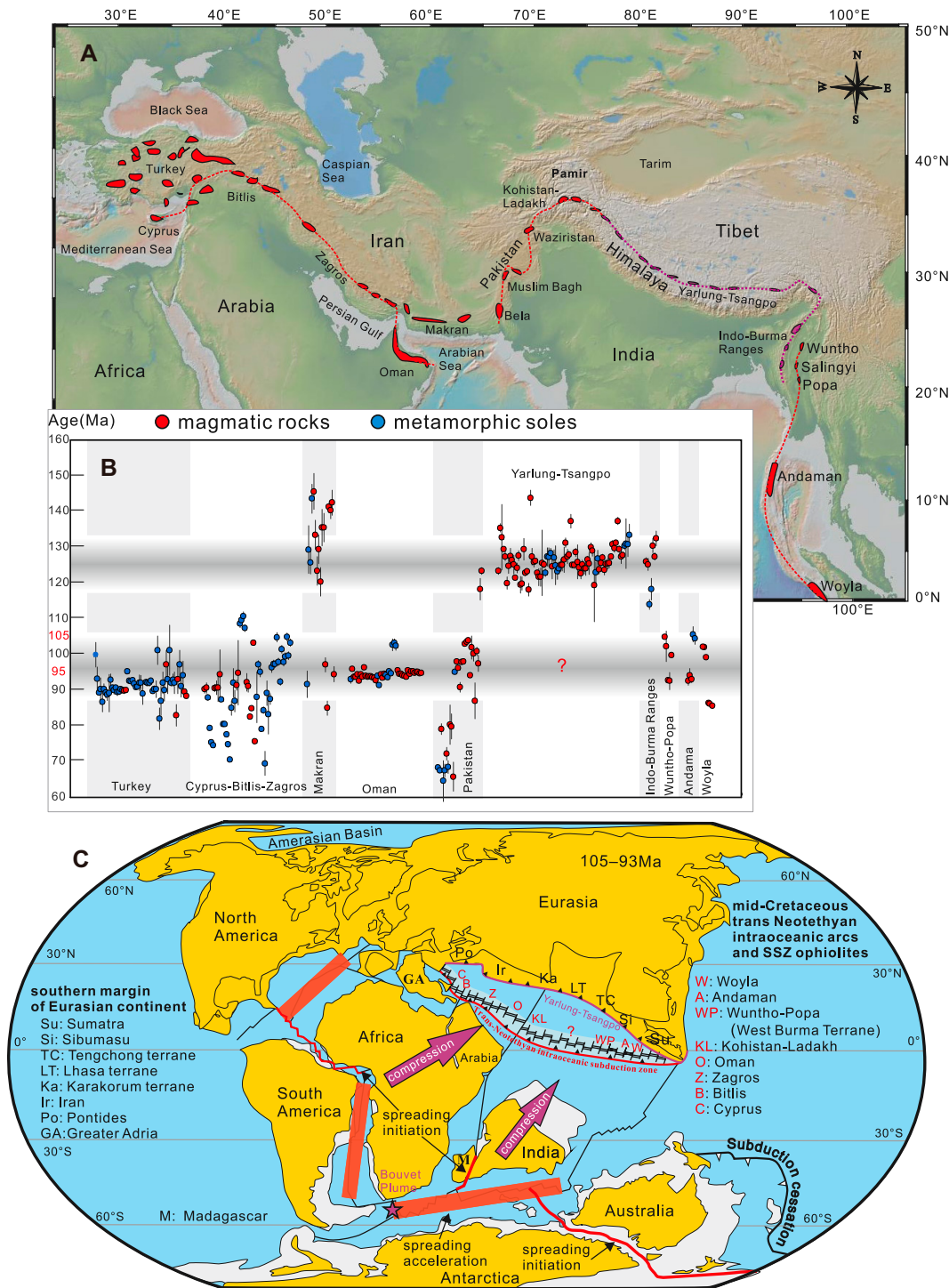


Figure 12. (A) E-W distributions of supra-subduction zone (SSZ) ophiolites and island arcs along eastern Mediterranean, Middle East, Pakistan, Himalaya-Tibet, western Myanmar, and Southeast Asia and (B) their formation ages for magmatic rocks and metamorphic soles. Data of the sampling localities, ages, and references are presented in Supporting Information Table S4 (see footnote 1). (C) Reconstruction of the trans-Neotethyan intraoceanic subduction system (after Hall, 2012; Jagoutz et al., 2015; Maffione et al., 2017; Matthews et al., 2012; van Hinsbergen et al., 2016, 2020; Westerweel et al., 2019). It is inferred that the Neotethyan mid-oceanic ridge became a convergent plate boundary driven by a global stress concentration during the mid-Cretaceous time and thus this inversion was probably triggered by final Gondwana breakup and global plate reorganization.

~20 m.y. has resulted in a maximum plate convergence of 150–200 km (Sutherland et al., 2006) and a depth of ~150 km for the leading edge of the Indian-Australian plate in the infant Benioff zone beneath the Pacific Plate where the self-sustaining state may have not yet been achieved (Gurnis et al., 2004, 2019; Mao et al., 2017). Noticeably, island arc calc-alkaline volcanic rocks are sparsely distributed

on the overriding plate (e.g., Solander Island; Reay and Parkinson, 1997).

In the above context, fertile asthenosphere may be trapped within the shallow mantle wedge according to our ridge inversion model (Fig. 11C). If true, island arc tholeiitic and calc-alkaline magmas could be produced by wet melting of this fertile mantle (M2) aided by hydrous fluids and pelagic sediment-derived melts

(Fig. 11C). The 105–93 Ma Mawgyi island arc tholeiites and calc-alkaline rocks would be interpreted here to have been generated in this geodynamic setting where the MORB-like and arc-like magmas are broadly coeval and spatially juxtaposed (Fig. 11C). This would indicate that the normal island arc magmatism can also account for building the earliest protoarc crust during intraoceanic subduction initiation. Analogically,

the young (ca. 2 Ma) initiation of the Matthew-Hunter infant subduction zone is characterized by an exceptionally diverse range of magmatic compositions (Patriat et al., 2019).

The Mawgyi MORB-like magmas exhibit noticeable geochemical signatures of subducted sediment-derived melt contributions (Figs. 9B–9D). This is in stark contrast with those of the IBM protoarc basalts. We speculate that rapid mantle upwelling relative to the heating rate of the cold, ancient Pacific oceanic slab (Reagan et al., 2010; Stern and Bloomer, 1992) or accretionary-type subduction during the earliest period (Li et al., 2019a) may have been required to minimize the subduction input for the IBM protoarc basalts. Ridge inversion along a detachment fault within the mid-Cretaceous Neotethys may have occurred in a nonaccretionary-type subduction zone where a younger and hotter slab was subducted (Fig. 11). As the thermal regime of the shallower subduction zone progressively cooled down, the eclogitic densification of the sinking slab would have started to contribute significantly to slab pull and ultimately reach self-sustaining subduction (e.g., Duisterhoef et al., 2014), leading to a deeper asthenospheric mantle wedge everywhere in mature subduction zones (like M3; Syracuse et al., 2010).

The Trigger for Mid-Cretaceous Inversion of the Neotethyan Mid-Oceanic Ridges

A major plate reorganization has been posited at 105–100 Ma (Fig. 12; Gibbons et al., 2015; Matthews et al., 2012). Final separation of South America and Africa in the Equatorial Atlantic Ocean was achieved at ca. 104 Ma (Heine and Brune, 2014). An abrupt increase in rate of divergence between Australia and Antarctica occurred at ca. 100 Ma (Brune et al., 2016; Müller et al., 2016; Plummer, 1996). Transform rifting between Madagascar and Seychelles, and a dextral trans-tension between Madagascar and India started at 100–95 Ma (Matthews et al., 2012; Plummer, 1996; Seton et al., 2012). Massive eruptions associated with the Bouvet Plume near the South American-African-Antarctic triple junction occurred between 100 Ma and 94 Ma and formed the Agulhas Plateau, Maud Rise, and Northeast Georgia Rise (Parsiegla et al., 2008). The Amerasian Basin in the western Arctic Ocean formed at 105–100 Ma (Mukasa et al., 2020). All the above events, in a short period of geologic time, incrementally increased the amount of global oceanic lithosphere which must have been largely compensated by recycling oceanic lithosphere back to the mantle through subduction. Coincidentally, a >7000-km-long west-dipping subduction zone ceased along the eastern margin of Gondwana at 105–100 Ma (Fig. 12C; Matthews et al., 2012).

The cessation of this subduction may have accelerated the Earth's imbalance globally between plate growth and consumption during the mid-Cretaceous. Enhanced convergence rates along the existing subduction zones at that time or initiating new subduction zones would correspond with accelerated plate consumption (e.g., Ulvrova et al., 2019). However, existing subduction zones may not always easily accommodate subduction acceleration due to the coupling between the subducting slabs and the high-viscosity ambient mantle, and instead this global imbalance may have initiated new subduction zones at some locations (Ulvrova et al., 2019). If the plates north of the Neotethyan spreading ridge accelerated less than the southern Indian-African plates, it is likely that the Neotethyan mid-oceanic ridge became a convergent plate boundary driven by a global stress concentration during the mid-Cretaceous (Fig. 12C). The cooccurrences of many Neotethyan SSZ ophiolites and extensive intraoceanic arcs (Figs. 12A and 12B) may represent the products of this mid-Cretaceous abrupt global plate reorganization. The >8000-km-long oceanic plate consumption along this trans-Neotethyan subduction system would account for the excess crust during the mid-Cretaceous Gondwana breakup events (Fig. 12C; Brune et al., 2016). Subduction initiation is probably a self-consistent outcome of plate convergence accompanying continental rifting and seafloor spreading, as any plate generation must be principally balanced by plate consumption on the constant Earth's surface (McKenzie, 1977). In other words, the abrupt and short-period of imbalance between plate growth and plate consumption on Earth is probably modulated through global plate reorganization.

CONCLUSION

The Mawgyi Volcanics, the oldest volcanic succession of the Wuntho-Salingyi-Popa arc straddling the West Burma Terrane, mainly consists of MORB-like rocks, subordinate island arc tholeiite and calc-alkaline lavas and dikes. The Mawgyi MORB-like rocks are characterized by flat REE patterns and depleted in abundance of REEs, HSFs (except for Th), and TiO_2 relative to those of the Indian MORBs, geochemically resembling the IBM protoarc basalts. Importantly, based on the discriminative Ti-V diagram, the Salingyi dolerites were produced at more reducing conditions than those of the Wuntho volcanic rocks. This implies that the Salingyi dolerites were probably intruded in a region close to the incipient slab edge, but farther than the Wuntho volcanic rocks. As such, the Wuntho and Salingyi in tectonic positions may correspond to the IBM forearc and the IODP

Site U1438 during subduction initiation, respectively. Our geochronological results show that the Mawgyi Volcanics formed between 105 Ma and 93 Ma. This coincided with the formation of many Neotethyan SSZ ophiolites and island arcs along the eastern Mediterranean, Middle East, Pakistan, and Southeast Asia. The Wuntho-Popa arc with near-equatorial paleo-latitudes (Westerweel et al., 2019) possibly formed part of a mid-Cretaceous trans-Neotethyan subduction system over 8000 km in length from west to east. Inversion of mid-oceanic ridges provides an appealing explanation for mid-Cretaceous subduction initiation within the Neotethys given the available evidence. Importantly, the higher Hf/Nd ratios of the Mawgyi MORB-like rocks indicate some input of altered oceanic crust melts (like the Salingyi rhyolites), which advocates partial melting of young, hot and infant oceanic slab during ridge inversion. This trans-Neotethyan intraoceanic subduction system was probably triggered by far afield forces associated with an abrupt global plate reorganization and compensated by an excess of plate generation during mid-Cretaceous breakup of the Gondwana supercontinent and a sudden stagnation of long-distance subduction zone along eastern margin of Gondwana (Matthews et al., 2012). If correct, this mid-Cretaceous near-equatorial intraoceanic subduction zone plus the contemporaneous subduction zone along the southernmost margin of the Asian continent, would define a double subduction system between India and Asia and better account for the fast convergence between Indian and Asian continents during the Late Cretaceous to Paleogene (Gibbons et al., 2015; Jagoutz et al., 2015; van Hinsbergen et al., 2011). Additionally, the Mawgyi MORB-like rocks with high Th/La ratios carry the noticeable signatures of sediment inputs indicating that this trans-Neotethyan subduction system was probably characterized by non- or low-accretionary subduction during subduction initiation through ridge inversion. The observations that the temporal simultaneity and spatial juxtaposition between the MORB-like and island arc tholeiitic and calc-alkaline magmas of the Mawgyi Volcanics, indicate that the normal island arc magmatism can emerge during subduction initiation, and much earlier than traditionally thought.

ACKNOWLEDGMENTS

We thank Shouqian Zhao, Yahui Yue and Yali Sun for their assistances with lab analysis, and Paul Kapp for feedback on an early version of this manuscript. This manuscript was further strengthened by constructive comments from Associate Editor Xixi Zhao and one anonymous reviewer, and suggestions by Science Editor Brad S. Singer. This research was funded by the Strategic Priority Research Program of Chinese Academy of Sciences (Grant No. XDA20070301).

the Second Tibetan Plateau Scientific Expedition and Research Program (Grant No. 2019QZKK0708), the National Natural Science Foundation Project (Grant No. 41490613 and 41490615), and the Ministry of Science and Technology of China (Grant No. 2016YFC0600303). M.N. Ducea acknowledges support from US National Science Foundation (Grant No. EAR 1725002) and the Romanian Executive Agency for Higher Education, Research, Development and Innovation Funding projects (Grant No. PN-III-P4-ID-PCCF-2016-0014).

REFERENCES CITED

- Abrajvitch, A., Ali, J., Aitchison, J., Badengzhu, Davis, A., Liu, J., and Ziabrev, S., 2005, Neotethys and the India-Asia collision: Insights from a palaeomagnetic study of the Dazhuqi ophiolite, southern Tibet: *Earth and Planetary Science Letters*, v. 233, p. 87–102, <https://doi.org/10.1016/j.epsl.2005.02.003>.
- Acharyya, S.K., 2015, Indo-Burma Range: A belt of accreted microcontinents, ophiolites and Mesozoic-Paleogene flyschoid sediments: *International Journal of Earth Sciences*, v. 104, p. 1235–1251, <https://doi.org/10.1007/s00531-015-1154-6>.
- Agard, P., Jolivet, L., Vrielynck, B., Burrov, E., and Monié, P., 2007, Plate acceleration: The obduction trigger?: *Earth and Planetary Science Letters*, v. 258, p. 428–441, <https://doi.org/10.1016/j.epsl.2007.04.002>.
- Agard, P., Yamato, P., Soret, M., Prigent, C., Guillot, S., Plunder, A., Dubacq, B., Chauvet, A., and Monie, P., 2016, Plate interface rheological switches during subduction infancy: Control on slab penetration and metamorphic sole formation: *Earth and Planetary Science Letters*, v. 451, p. 208–220, <https://doi.org/10.1016/j.epsl.2016.06.054>.
- Ahmad, M.N., Yoshida, M., and Fujiwara, Y., 2000, Paleomagnetic study of Utror Volcanic Formation: Remagnetization and postfolding rotations in Utror area, Kohistan arc, northern Pakistan: *Earth, Planets, and Space*, v. 52, p. 425–436, <https://doi.org/10.1186/BF03325254>.
- Aitchison, J., McDermid, I., Ali, J., Davis, A., and Zybrev, S., 2007, Shoshonites in southern Tibet record Late Jurassic rifting of a Tethyan intraoceanic island arc: *The Journal of Geology*, v. 115, p. 197–213, <https://doi.org/10.1086/510642>.
- Aitchison, J.C., Davis, A.M., Liu, J., Luo, H., Malpas, J.G., McDermid, I.R., McDermid, I.R.C., Wu, H.Y., Ziabrev, S.V., and Zhou, M.F., 2000, Remnants of a Cretaceous intra-oceanic subduction system within the Yarlung-Zangbo suture (southern Tibet): *Earth and Planetary Science Letters*, v. 183, p. 231–244, [https://doi.org/10.1016/S0012-821x\(00\)00287-9](https://doi.org/10.1016/S0012-821x(00)00287-9).
- Andersen, T., 2002, Correction of common lead in U-Pb analyses that do not report ^{204}Pb : *Chemical Geology*, v. 192, p. 59–79, [https://doi.org/10.1016/S0009-2541\(02\)00195-X](https://doi.org/10.1016/S0009-2541(02)00195-X).
- Arculus, R.J., Ishizuka, O., Bogus, K.A., Gurnis, M., Hickey-Vargas, R., Aljehdali, M.H., Bandini-Maeder, A.N., Barth, A.P., Brandl, P.A., Drab, L., do Monte Guerra, R., Hamada, M., Jiang, F., Kanayama, K., Kender, S., Kusano, Y., Li, H., Loudin, L.C., Maffione, M., Marsaglia, K.M., McCarthy, A., Meffre, S., Morris, A., Neuhäus, M., Savov, I.P., Sena, C., Tepley, F.J., van der Land, C., Yagodinski, G.M., and Zhang, Z., 2015, A record of spontaneous subduction initiation in the Izu-Bonin-Mariana arc: *Nature Geoscience*, v. 8, p. 728–733, <https://doi.org/10.1038/ngeo2515>.
- Beaussier, S.J., Gerya, T.V., and Burg, J.-P., 2019, Near-ridge initiation of intraoceanic subduction: Effects of inheritance in 3D numerical models of the Wilson Cycle: *Tectonophysics*, v. 763, p. 1–13, <https://doi.org/10.1016/j.tecto.2019.04.011>.
- Bouilhol, P., Jagoutz, O., Hanchar, J.M., and Dudas, F.O., 2013, Dating the India-Eurasia collision through arc magmatic records: *Earth and Planetary Science Letters*, v. 366, p. 163–175, <https://doi.org/10.1016/j.epsl.2013.01.023>.
- Brounce, M., Kelley, K.A., Cottrell, E., and Reagan, M.K., 2015, Temporal evolution of mantle wedge oxygen fugacity during subduction initiation: *Geology*, v. 43, p. 775–778, <https://doi.org/10.1130/G36742.1>.
- Brune, S., Williams, S.E., Butterworth, N.P., and Muller, R.D., 2016, Abrupt plate accelerations shape rifted continental margins: *Nature*, v. 536, p. 201–204, <https://doi.org/10.1038/nature18319>.
- Burg, J.P., 2011, The Asia-Kohistan-India collision: Review and discussion, in Brown, D., and Ryan, P.D., eds., *Arc-Continent Collision*: Berlin, Heidelberg, Germany, Springer, p. 279–309, https://doi.org/10.1007/978-3-540-88558-0_10.
- Butler, J.P., and Beaumont, C., 2017, Subduction zone decoupling/retreat modeling explains south Tibet (Xigaze) and other supra-subduction zone ophiolites and their UHP mineral phases: *Earth and Planetary Science Letters*, v. 463, p. 101–117, <https://doi.org/10.1016/j.epsl.2017.01.025>.
- Cai, F.L., Ding, L., Zhang, Q.H., Orme, D.A., Wei, H.H., Li, J.X., Zhang, J.E., Zaw, T., and Sein, K., 2019, Initiation and evolution of forearc basins in the Central Myanmar Depression: *Geological Society of America Bulletin*, v. 132, p. 1066–1082, <https://doi.org/10.1130/B35301.1>.
- Casey, J.F., and Dewey, J.F., 1984, Initiation of subduction zones along transform and accreting plate boundaries, triple-junction evolution, and forearc spreading centres: Implications for ophiolitic geology and obduction, in Gass, I.G., Lippard, S.L., and Shelton, A.W., eds., *Ophiolites and Oceanic Lithosphere*: Geological Society of London, Special Publications, v. 13, p. 269–290, <https://doi.org/10.1144/GSL.SP.1984.013.01.22>.
- Cloos, M., 1993, Lithospheric buoyancy and collisional orogenesis: Subduction of oceanic plateaus, continental margins, island arcs, spreading ridges, and seamounts: *Geological Society of America Bulletin*, v. 105, no. 6, [https://doi.org/10.1130/0016-7606\(1993\)105<0715:LBACOS>2.3.CO;2](https://doi.org/10.1130/0016-7606(1993)105<0715:LBACOS>2.3.CO;2).
- Corfield, R.I., Searle, M.P., and Pedersen, R.B., 2001, Tectonic setting, origin, and obduction history of the Spontang ophiolite, Ladakh Himalaya, NW India: *The Journal of Geology*, v. 109, p. 715–736, <https://doi.org/10.1086/323191>.
- Coulthard, D.A.J., Reagan, M.K., Almeev, R., Pearce, J.A., Ryan, J., Sakuyama, T., Shervais, J.W., and Shimizu, K., 2017, Fore-arc basalt to boninite magmatism: Characterizing the transition from decompression to fluid flux melting after subduction initiation: *Geological Society of America Abstracts with Programs*, v. 49, no. 6, <https://doi.org/10.1130/abs/2017AM-305866>.
- Curray, J.R., 2005, Tectonics and history of the Andaman Sea region: *Journal of Asian Earth Sciences*, v. 25, no. 1, p. 187–228, <https://doi.org/10.1016/j.jseaes.2004.09.001>.
- Dai, J., Wang, C., Polat, A., Santosh, M., Li, Y., and Ge, Y., 2013, Rapid forearc spreading between 130 and 120 Ma: Evidence from geochronology and geochemistry of the Xigaze ophiolite, southern Tibet: *Lithos*, v. 172–173, p. 1–16, <https://doi.org/10.1016/j.lithos.2013.03.011>.
- DeBari, S.M., Taylor, B., Spencer, K., and Fujioka, K., 1999, A trapped Philippine Sea plate origin for MORB from the inner slope of the Izu-Bonin trench: *Earth and Planetary Science Letters*, v. 174, p. 183–197, [https://doi.org/10.1016/S0012-821X\(99\)00252-6](https://doi.org/10.1016/S0012-821X(99)00252-6).
- Dilek, Y., and Furnes, H., 2011, Ophiolite genesis and global tectonics: Geochemical and tectonic fingerprinting of ancient oceanic lithosphere: *Geological Society of America Bulletin*, v. 123, p. 387–411, <https://doi.org/10.1130/B30446.1>.
- Dilek, Y., and Thy, P., 2009, Island arc tholeiite to boninitic melt evolution of the Cretaceous Kizildag (Turkey) ophiolite: Model for multi-stage early arc-forearc magmatism in Tethyan subduction factories: *Lithos*, v. 113, p. 68–87, <https://doi.org/10.1016/j.lithos.2009.05.044>.
- Ducea, M.N., Saleeby, J.B., and Bergantz, G., 2015, The Architecture, Chemistry, and Evolution of Continental Magmatic Arcs: *Annual Review of Earth and Planetary Sciences*, v. 43, p. 299–331, <https://doi.org/10.1146/annurev-earth-060614-105049>.
- Duesterhoeft, E., Quinteros, J., Oberhänsli, R., Bousquet, R., and de Capitani, C., 2014, Relative impact of mantle densification and eclogitization of slabs on subduction dynamics: A numerical thermodynamic/thermokinematic investigation of metamorphic density evolution: *Tectonophysics*, v. 637, p. 20–29, <https://doi.org/10.1016/j.tecto.2014.09.009>.
- Escartín, J., Smith, D.K., Cann, J., Schouten, H., Langmuir, C.H., and Escrig, S., 2008, Central role of detachment faults in accretion of slow-spreading oceanic lithosphere: *Nature*, v. 455, p. 790–794, <https://doi.org/10.1038/nature07333>.
- Fareeduddin, and Dilek, Y., 2015, Structure and petrology of the Nagaland-Manipur Hill Ophiolitic Mélange zone, NE India: A fossil Tethyan subduction channel at the India-Burma plate boundary: *Episodes*, v. 38, p. 298–314, <https://doi.org/10.18814/epiuius/2015/v38i4/82426>.
- Forsyth, D., and Uyeda, S., 1975, On the relative importance of the driving forces of plate motion: *Geophysical Journal International*, v. 43, p. 163–200, <https://doi.org/10.1111/j.1365-246X.1975.tb00631.x>.
- Gahalaut, V.K., and Gahalaut, K., 2007, Burma plate motion: *Journal of Geophysical Research. Solid Earth*, v. 112, no. B10, <https://doi.org/10.1029/2007JB004928>.
- Gale, A., Dalton, C.A., Langmuir, C.H., Su, Y., and Schilling, J.-G., 2013, The mean composition of ocean ridge basalts: *Geochemistry, Geophysics, Geosystems*, v. 14, p. 489–518, <https://doi.org/10.1029/2012GC004334>.
- Gardiner, N.J., Hawkesworth, C.J., Robb, L.J., Whitehouse, M.J., Roberts, N.M.W., Kirkland, C.L., and Evans, N.J., 2017, Contrasting granite metallogeny through the zircon record: A case study from Myanmar: *Scientific Reports*, v. 7, no. 748, <https://doi.org/10.1038/s41598-017-00832-2>.
- Garrido, C.J., Bodinier, J.L., Dhuime, B., Bosch, D., Chanefo, I., Bruguier, O., Hussain, S.S., Dawood, H., and Burg, J.P., 2007, Origin of the island arc Moho transition zone via melt-rock reaction and its implications for intracrustal differentiation of island arcs: Evidence from the Jijal complex (Kohistan complex, northern Pakistan): *Geology*, v. 35, no. 8, p. 683–686, <https://doi.org/10.1130/G23675A.1>.
- Gibbons, A.D., Zahirovic, S., Muller, R.D., Whittaker, J.M., and Yatheesh, V., 2015, A tectonic model reconciling evidence for the collisions between India, Eurasia and intra-oceanic arcs of the central-eastern Tethys: *Gondwana Research*, v. 28, p. 451–492, <https://doi.org/10.1016/j.gr.2015.01.001>.
- Green, E.C.R., White, R.W., Diener, J.F.A., Powell, R., Holland, T.J.B., and Palin, R.M., 2016, Activity-composition relations for the calculation of partial melting equilibria in metabasic rocks: *Journal of Metamorphic Geology*, v. 34, p. 845–869, <https://doi.org/10.1111/jmg.12211>.
- Grove, T., Chatterjee, N., Parman, S., and Medard, E., 2006, The influence of H₂O on mantle wedge melting: *Earth and Planetary Science Letters*, v. 249, p. 74–89, <https://doi.org/10.1016/j.epsl.2006.06.043>.
- Guilmette, C., Hebert, R., Dostal, J., Indares, A., Ullrich, T., Bernard, E., and Wang, C.S., 2012, Discovery of a dismembered metamorphic sole in the Saga ophiolitic mélange, South Tibet: Assessing an Early Cretaceous disruption of the Neo-Tethyan supra-subduction zone and consequences on basin closing: *Gondwana Research*, v. 22, no. 2, p. 398–414, <https://doi.org/10.1016/j.gr.2011.10.012>.
- Guilmette, C., Smit, M.A., van Hinsbergen, D.J.J., Güler, D., Corfu, F., Charette, B., Maffione, M., Rabeau, O., and Savard, D., 2018, Forced subduction initiation recorded in the sole and crust of the Semail Ophiolite of Oman: *Nature Geoscience*, v. 11, p. 688–695, <https://doi.org/10.1038/s41561-018-0209-2>.
- Gülcher, A.J.P., Beaussier, S.J., and Gerya, T.V., 2019, On the formation of oceanic detachment faults and their influence on intra-oceanic subduction initiation: 3D thermomechanical modeling: *Earth and Planetary Science Letters*, v. 506, p. 195–208, <https://doi.org/10.1016/j.epsl.2018.10.042>.
- Gurnis, M., Hall, C., and Lavier, L., 2004, Evolving force balance during incipient subduction: *Geochemistry, Geophysics, Geosystems*, v. 5, no. 7, <https://doi.org/10.1029/2003GC000681>.

- Gurnis, M., van Avendonk, H., Gulick, S.P.S., Stock, J., Sutherland, R., Hightower, E., Shuck, B., Patel, J., Williams, E., Kardell, D., Herzog, E., Idini, B., Graham, K., Estep, J., and Carrington, L., 2019, Incipient subduction at the contact with stretched continental crust: The Puysegur Trench: *Earth and Planetary Science Letters*, v. 520, p. 212–219, <https://doi.org/10.1016/j.epsl.2019.05.044>.
- Haase, K.M., Freund, S., Koepke, J., Hauff, F., and Erdmann, M., 2015, Melts of sediments in the mantle wedge of the Oman ophiolite: *Geology*, v. 43, p. 275–278, <https://doi.org/10.1130/G36451.1>.
- Hacker, B.R., Mosenfelder, J.L., and Gnos, E., 1996, Rapid emplacement of the Oman ophiolite, Thermal and geochronologic constraints: *Tectonics*, v. 15, p. 1230–1247, <https://doi.org/10.1029/96TC01973>.
- Hall, C.E., Gurnis, M., Sdrolias, M., Lavie, L.L., and Müller, R.D., 2003, Catastrophic initiation of subduction following forced convergence across fracture zones: *Earth and Planetary Science Letters*, v. 212, p. 15–30, [https://doi.org/10.1016/S0012-821X\(03\)00242-5](https://doi.org/10.1016/S0012-821X(03)00242-5).
- Hall, R., 2012, Late Jurassic-Cenozoic reconstructions of the Indonesian region and the Indian Ocean: *Tectonophysics*, v. 570–571, p. 1–41, <https://doi.org/10.1016/j.tecto.2012.04.021>.
- Haugen, E., 2017, Magmatic evolution of early subduction zones: Geochemical modeling and chemical stratigraphy of boninite and fore arc basalt from the Bonin fore arc [M.S. thesis]: Logan, Utah, USA, Utah State University, 166 p., <https://digitalcommons.usu.edu/etd/5934/>.
- Hébert, R., Bezard, R., Guilmette, C., Dostal, J., Wang, C.S., and Liu, Z.F., 2012, The Indus-Yarlung Zangbo ophiolites from Nanga Parbat to Namche Barwa syntaxes, southern Tibet: First synthesis of petrology, geochemistry, and geochronology with incidences on geodynamic reconstructions of Neo-Tethys: *Gondwana Research*, v. 22, p. 377–397, <https://doi.org/10.1016/j.gr.2011.10.013>.
- Heine, C., and Brune, S., 2014, Oblique rifting of the Equatorial Atlantic: Why there is no Saharan Atlantic Ocean: *Geology*, v. 42, p. 211–214, <https://doi.org/10.1130/G35082.1>.
- Hickey-Vargas, R., 1998, Origin of the Indian Ocean-type isotopic signature in basalts from Philippine Sea plate spreading centers: An assessment of local versus large-scale processes: *Journal of Geophysical Research*. *Solid Earth*, v. 103, p. 20963–20979, <https://doi.org/10.1029/98JB02052>.
- Hickey-Vargas, R., Yagodinski, G.M., Ishizuka, O., McCarthy, A., Bizimis, M., Kusano, Y., Savov, I.P., and Arculus, R., 2018, Origin of depleted basalts during subduction initiation and early development of the Izu-Bonin-Mariana island arc: Evidence from IODP expedition 351 site U1438, Amami-Sankaku basin: *Geochimica et Cosmochimica Acta*, v. 229, p. 85–111, <https://doi.org/10.1016/j.gca.2018.03.007>.
- Hirschmann, M.M., Ghiorso, M.S., Wasylenki, L.E., Asimow, P.D., and Stolper, E.M., 1998, Calculation of peridotite partial melting from thermodynamic models of minerals and melts. I. Review of methods and comparison with experiments: *Journal of Petrology*, v. 39, p. 1091–1115, <https://doi.org/10.1093/ptro/j/39.6.1091>.
- Htay, H., Zaw, K., and Oo, T.T., 2017, The mafic-ultramafic (ophiolitic) rocks of Myanmar, in Barber, A.J., Khin, Z., and Crow, M.J., eds., Myanmar: Geology, Resources and Tectonics: Geological Society of London Memoirs, v. 48, p. 117–141, <https://doi.org/10.1144/M48.6>.
- Huang, W., van Hinsbergen, D.J.J., Maffione, M., Orme, D.A., Dupont-Nivet, G., Guilmette, C., Ding, L., Guo, Z., and Kapp, P., 2015, Lower Cretaceous Xigaze ophiolites formed in the Gangdese forearc: Evidence from paleomagnetism, sediment provenance, and stratigraphy: *Earth and Planetary Science Letters*, v. 415, p. 142–153, <https://doi.org/10.1016/j.epsl.2015.01.032>.
- Huang, H., Pérez-Pinedo, D., Morley, R.J., Dupont-Nivet, G., Philip, A., Win, Z., Aung, D.W., Licht, A., Jardine, P.E., and Hoorn, C., 2021, At a crossroads: The late Eocene flora of central Myanmar owes its composition to plate collision and tropical climate: Review of Palaeobotany and Palynology, <https://doi.org/10.1016/j.revpalbo.2021.104441>.
- Humphris, S.E., and Thompson, G., 1978, Trace-element mobility during hydrothermal alteration of oceanic basalts: *Geochimica et Cosmochimica Acta*, v. 42, p. 127–136, [https://doi.org/10.1016/0016-7037\(78\)90222-3](https://doi.org/10.1016/0016-7037(78)90222-3).
- Ishizuka, O., Tani, K., Reagan, M.K., Kanayama, K., Umino, S., Harigane, Y., Sakamoto, I., Miyajima, Y., Yuasa, M., and Dunkley, D.J., 2011a, The timescales of subduction initiation and subsequent evolution of an oceanic island arc: *Earth and Planetary Science Letters*, v. 306, p. 229–240, <https://doi.org/10.1016/j.epsl.2011.04.006>.
- Ishizuka, O., Taylor, R.N., Yuasa, M., and Ohara, Y., 2011b, Making and breaking an island arc: A new perspective from the Oligocene Kyushu-Palau arc, Philippine Sea: *Geochemistry, Geophysics, Geosystems*, v. 12, no. 5, <https://doi.org/10.1029/2010GC003440>.
- Ishizuka, O., Hickey-Vargas, R., Arculus, R.J., Yagodinski, G.M., Savov, I.P., Kusano, Y., McCarthy, A., Brandl, P.A., and Sudo, M., 2018, Age of Izu-Bonin-Mariana arc basement: *Earth and Planetary Science Letters*, v. 481, p. 80–90, <https://doi.org/10.1016/j.epsl.2017.10.023>.
- Iwamori, H., 1998, Transportation of H₂O and melting in subduction zones: *Earth and Planetary Science Letters*, v. 160, p. 65–80, [https://doi.org/10.1016/S0012-821X\(98\)00080-6](https://doi.org/10.1016/S0012-821X(98)00080-6).
- Jagoutz, O., Royden, L., Holt, A.F., and Becker, T.W., 2015, Anomalously fast convergence of India and Eurasia caused by double subduction: *Nature Geoscience*, v. 8, p. 475–478, <https://doi.org/10.1038/ngeo2418>.
- Jagoutz, O., Bouilhol, P., Schaltegger, U., and Müntener, O., 2019, The isotopic evolution of the Kohistan Ladakh arc from subduction initiation to continent arc collision, in Treloar, P.J., and Searle, M.P., eds., Himalayan Tectonics: A Modern Synthesis: Geological Society of London, Special Publications, v. 483, no. 1, p. 165–182, <https://doi.org/10.1144/SP483.7>.
- Kanayama, K., Umino, S., and Ishizuka, O., 2012, Eocene volcanism during the incipient stage of Izu-Ogasawara Arc: Geology and petrology of the Mukojima Island Group, the Ogasawara Islands: *The Island Arc*, v. 21, p. 288–316, <https://doi.org/10.1111/iar.12000>.
- Kanayama, K., Kitamura, K., and Umino, S., 2013, New geochemical classification of global boninites: International Association of Volcanology and Chemistry of the Earth's Interior 2013 Scientific Assembly, 20–24 July, Kagoshima, Japan, p. 99.
- Kapp, P., and DeCelles, P.G., 2019, Mesozoic-Cenozoic geological evolution of the Himalayan-Tibetan orogen and working tectonic hypotheses: *American Journal of Science*, v. 319, p. 159–254, <https://doi.org/10.2475/03.2019.01>.
- Keenan, T.E., Encarnacion, J., Buchwaldt, R., Fernandez, D., Mattinson, J., Rasoazanamparany, C., and Lutetkemeyer, P.B., 2016, Rapid conversion of an oceanic spreading center to a subduction zone inferred from high-precision geochronology: *Proceedings of the National Academy of Sciences of the United States of America*, v. 113, p. 7359–7366, <https://doi.org/10.1073/pnas.1609999113>.
- Khan, M.A., Stern, R.J., Gribble, R.F., and Windley, B.F., 1997, Geochemical and isotopic constraints on subduction polarity, magma sources, and palaeogeography of the Kohistan intra-oceanic arc, northern Pakistan Himalaya: *Journal of the Geological Society*, v. 154, p. 935–946, <https://doi.org/10.1144/gsjgs.154.6.0935>.
- Khan, S.D., Walker, D.J., Hall, S.A., Burke, K.C., Shah, M.T., and Stockli, L., 2009, Did the Kohistan-Ladakh island arc collide first with India? *Geological Society of America Bulletin*, v. 121, p. 366–384, <https://doi.org/10.1130/B26348.1>.
- Klootwijk, C., Sharma, M.L., Gergan, J., Shah, S.K., and Tirkey, B., 1984, The Indus-Tsangpo suture zone in Ladakh, northwest Himalaya: Further palaeomagnetic data and implications: *Tectonophysics*, v. 106, p. 215–238, [https://doi.org/10.1016/0040-1951\(84\)90178-1](https://doi.org/10.1016/0040-1951(84)90178-1).
- Kusano, Y., Umino, S., Shinjo, R., Ikei, A., Adachi, Y., Miyashita, S., and Arai, S., 2017, Contribution of slab-derived fluid and sedimentary melt in the incipient arc magmas with development of the paleo-arc in the Oman Ophiolite: *Chemical Geology*, v. 449, p. 206–225, <https://doi.org/10.1016/j.chemgeo.2016.12.012>.
- Langmuir, C.H., Bezos, A., Escrig, S., and Parman, S.W., 2006, Chemical systematics and hydrous melting of the mantle in back-arc basins, in Givens, S., Christie, D.M., Fisher, C.R., and Lee, S.-M., eds., Back-Arc Spreading Systems: Geological, Biological, Chemical, and Physical Interactions: Washington, D.C., USA, American Geophysical Union, Geophysical Monograph Series, v. 166, p. 87–146, <https://doi.org/10.1029/166GM07>.
- Laskowski, A.K., Orme, D.A., Cai, F., and Ding, L., 2019, The Ancestral Lhasa River: A Late Cretaceous trans-arc river that drained the proto-Tibetan Plateau: *Geology*, v. 47, p. 1029–1033, <https://doi.org/10.1130/G46823.1>.
- Lee, C.-T.A., Luffi, P., Plank, T., Dalton, H., and Lee-man, W.P., 2009, Constraints on the depths and temperatures of basaltic magma generation on Earth and other terrestrial planets using new thermobarometers for mafic magmas: *Earth and Planetary Science Letters*, v. 279, p. 20–33, <https://doi.org/10.1016/j.epsl.2008.12.020>.
- Leng, W., and Gurnis, M., 2011, Dynamics of subduction initiation with different evolutionary pathways: *Geochemistry, Geophysics, Geosystems*, v. 12, no. 12, <https://doi.org/10.1029/2011GC003877>.
- Li, H.-Y., Taylor, R.N., Prytulak, J., Kirchenbaun, M., Shervais, J.W., Ryan, J.G., Godard, M., Reagan, M.K., and Pearce, J.A., 2019a, Radiogenic isotopes document the start of subduction in the Western Pacific: *Earth and Planetary Science Letters*, v. 518, p. 197–210, <https://doi.org/10.1016/j.epsl.2019.04.041>.
- Li, J.-X., Fan, W.-M., Zhang, L.-Y., Evans, N.J., Sun, Y.-L., Ding, L., Guan, Q.-Y., Peng, T.-P., Cai, F.-L., and Sein, K., 2019b, Geochronology, geochemistry and Sr-Nd-Hf isotopic compositions of Late Cretaceous-Eocene granites in southern Myanmar: Petrogenetic, tectonic and metallogenic implications: *Ore Geology Reviews*, v. 112, <https://doi.org/10.1016/j.oregeorev.2019.103031>.
- Li, J.-X., Fan, W.-M., Zhang, L.-Y., Peng, T.-P., Sun, Y.-L., Ding, L., Cai, F.-L., and Sein, K., 2020a, Prolonged Neo-Tethyan magmatic arc in Myanmar: Evidence from geochemistry and Sr-Nd-Hf isotopes of Cretaceous mafic-felsic intrusions in the Banmauk-Kawlin area: *International Journal of Earth Sciences*, v. 109, p. 649–668, <https://doi.org/10.1007/s00531-020-01824-w>.
- Li, S., Chung, S.-L., Lai, Y.-M., Ghani, A.A., Lee, H.-Y., and Murtagha, S., 2020b, Mesozoic juvenile crustal formation in the easternmost Tethys: Zircon Hf isotopic evidence from Sumatran granitoids, Indonesia: *Geology*, v. 48, no. 10, p. 1002–1005, <https://doi.org/10.1130/G47304.1>.
- Licht, A., Dupont-Nivet, G., Win, Z., Swe, H.H., Kaythi, M., Roperch, P., Ugrai, T., Littell, V., Park, D., Westerkemper, J., Jones, D., Poblete, F., Aung, D.W., Huang, H., Hoorn, C., and Sein, K., 2018, Paleogene evolution of the Burmese forearc basin and implications for the history of India-Asia convergence: *Geological Society of America Bulletin*, v. 131, p. 730–748, <https://doi.org/10.1130/B35002.1>.
- Lin, T.-H., Mitchell, A.H.G., Chung, S.-L., Tan, X.-B., Tang, J.-T., Oo, T., and Wu, F.-Y., 2019, Two parallel magmatic belts with contrasting isotopic characteristics from southern Tibet to Myanmar: zircon U-Pb and Hf isotopic constraints: *Journal of the Geological Society*, v. 176, p. 574–587, <https://doi.org/10.1144/jgs2018-072>.
- Liu, C.-Z., Chung, S.-L., Wu, F.-Y., Zhang, C., Xu, Y., Wang, J.-G., Chen, Y., and Guo, S., 2016a, Tethyan suturing in Southeast Asia: Zircon U-Pb and Hf-O isotopic constraints from Myanmar ophiolites: *Geology*, v. 44, p. 311–314, <https://doi.org/10.1130/G37342.1>.
- Liu, T., Wu, F.Y., Zhang, L.L., Zhai, Q.G., Liu, C.Z., Zhang, C., and Xu, Y., 2016b, Zircon U-Pb geochronological constraints on rapid exhumation of the mantle peridotite of the Xigaze ophiolite, southern Tibet: *Chemical Geology*, v. 443, p. 67–86, <https://doi.org/10.1016/j.chemgeo.2016.09.015>.

- Ludwig, K.R., 2003, User's Manual for Isoplot 3.00: A Geochronological Toolkit for Microsoft Excel: Berkeley Geochronology Center Special Publication, v. 4, 70 p.
- MacLeod, C.J., Escartin, J., Banerji, D., Banks, G.J., Gleeson, M., Irving, D.H.B., Lilly, R.M., McCaig, A.M., Niu, Y., Allerton, S., and Smith, D.K., 2002, Direct geological evidence for oceanic detachment faulting: The Mid-Atlantic Ridge, 15°45'N: *Geology*, v. 30, no. 10, [https://doi.org/10.1130/0091-7613\(2002\)030<0879:DGFEOD>2.0.CO;2](https://doi.org/10.1130/0091-7613(2002)030<0879:DGFEOD>2.0.CO;2).
- Maffione, M., van Hinsbergen, D.J.J., Koornneef, L.M.T., Guilmette, C., Hodges, K., Borneman, N., Huang, W.T., Ding, L., and Kapp, P., 2015a, Forearc hyperextension dismembered the south Tibetan ophiolites: *Geology*, v. 43, no. 6, p. 475–478, <https://doi.org/10.1130/G36472.1>.
- Maffione, M., Thieulot, C., van Hinsbergen, D.J.J., Morris, A., Plümmer, O., and Spakman, W., 2015b, Dynamics of intraoceanic subduction initiation: 1. Oceanic detachment fault inversion and the formation of supra-subduction zone ophiolites: *Geochemistry, Geophysics, Geosystems*, v. 16, p. 1753–1770, <https://doi.org/10.1002/2015GC005746>.
- Maffione, M., van Hinsbergen, D.J.J., de Gelder, G.I.N.O., van der Goes, F.C., and Morris, A., 2017, Kinematics of Late Cretaceous subduction initiation in the Neo-Tethys Ocean reconstructed from ophiolites of Turkey, Cyprus, and Syria: *Journal of Geophysical Research*, *Solid Earth*, v. 122, p. 3953–3976, <https://doi.org/10.1002/2016JB013821>.
- Mahéo, G., Bertrand, H., Guillot, S., Villa, I.M., Keller, F., and Capiez, P., 2004, The South Ladakh ophiolites (NW Himalaya, India): An intra-oceanic tholeiitic arc origin with implication for the closure of the Neo-Tethys: *Chemical Geology*, v. 203, p. 273–303, <https://doi.org/10.1016/j.chemgeo.2003.10.007>.
- Mahoney, J.J., Frei, R., Tejada, M., Mo, X., Leat, P., and Nägler, T., 1998, Tracing the Indian Ocean mantle domain through time: Isotopic results from old West Indian, East Tethyan, and South Pacific seafloor: *Journal of Petrology*, v. 39, p. 1285–1306, <https://doi.org/10.1093/ptro/39.7.1285>.
- Mao, X., Gurnis, M., and May, D.A., 2017, Subduction initiation with vertical lithospheric heterogeneities and new fault formation: *Geophysical Research Letters*, v. 44, p. 11349–11356, <https://doi.org/10.1002/2017GL075389>.
- Martin, C.R., Jagoutz, O., Upadhyay, R., Royden, L.H., Eddy, M.P., Bailey, E., Nichols, C.I.O., and Weiss, B.P., 2020, Paleocene latitude of the Kohistan-Ladakh arc indicates multistage India-Eurasia collision: *Proceedings of the National Academy of Sciences of the United States of America*, v. 117, no. 47, p. 29,487–29,494, <https://doi.org/10.1073/pnas.2009039117>.
- Matthews, K.J., Seton, M., and Müller, R.D., 2012, A global-scale plate reorganization event at 105 – 100 Ma: *Earth and Planetary Science Letters*, v. 355–356, p. 283–298, <https://doi.org/10.1016/j.epsl.2012.08.023>.
- Maunder, B., Prytulak, J., Goes, S., and Reagan, M., 2020, Rapid subduction initiation and magmatism in the Western Pacific driven by internal vertical forces: *Nature Communications*, v. 11, no. 1874, <https://doi.org/10.1038/s41467-020-15737-4>.
- McKenzie, D.P., 1977, The initiation of trenches: A finite amplitude instability, in Talwani, M., and Pitman, W.C., eds., *Island Arcs, Deep Sea Trenches and Back-Arc Basins*, Maurice Ewing Series 1: Washington, D.C., USA, American Geophysical Union, p. 57–61, <https://doi.org/10.1029/ME001p0057>.
- Mitchell, A., 2018, Geological Belts, Plate Boundaries, and Mineral Deposits in Myanmar: Oxford, UK, Elsevier, 509 p., <https://doi.org/10.1016/B978-0-12-803382-1.00004-3>.
- Mitchell, A., Chung, S.-L., Oo, T., Lin, T.-H., and Hung, C.-H., 2012, Zircon U-Pb ages in Myanmar: Magmatic-metamorphic events and the closure of a neo-Tethys ocean?: *Journal of Asian Earth Sciences*, v. 56, p. 1–23, <https://doi.org/10.1016/j.jseaes.2012.04.019>.
- Mitchell, A.H.G., 1992, Late Permian-Mesozoic events and the Mergui group Nappe in Myanmar and Thailand: *Journal of Southeast Asian Earth Sciences*, v. 7, p. 165–178, [https://doi.org/10.1016/0743-9547\(92\)90051-C](https://doi.org/10.1016/0743-9547(92)90051-C).
- Mitchell, A.H.G., 1993, Cretaceous-Cenozoic Tectonic Events in the Western Myanmar (Burma) Assam Region: *Journal of the Geological Society*, v. 150, p. 1089–1102, <https://doi.org/10.1144/gsjgs.150.6.1089>.
- Moghadam, H.S., and Stern, R.J., 2015, Ophiolites of Iran: Keys to understanding the tectonic evolution of SW Asia: (II) Mesozoic ophiolites: *Journal of Asian Earth Sciences*, v. 100, p. 31–59, <https://doi.org/10.1016/j.jseaes.2014.12.016>.
- Morley, C.K., 2012, Late Cretaceous–Early Palaeogene tectonic development of SE Asia: *Earth-Science Reviews*, v. 115, p. 37–75, <https://doi.org/10.1016/j.earscirev.2012.08.002>.
- Morley, C.K., and Arboit, F., 2019, Dating the onset of motion on the Sagaing fault: Evidence from detrital zircon and titanite U-Pb geochronology from the North Minwun Basin, Myanmar: *Geology*, v. 47, p. 581–585, <https://doi.org/10.1130/G46321.1>.
- Morley, C.K., Naing, T.T., Searle, M., and Robinson, S.A., 2020, Structural and tectonic development of the Indo-Burma ranges: *Earth-Science Reviews*, v. 200, no. 102992, <https://doi.org/10.1016/j.earscirev.2019.102992>.
- Mueller, S., and Phillips, R.J., 1991, On the initiation of subduction: *Journal of Geophysical Research*, *Solid Earth*, v. 96, p. 651–665, <https://doi.org/10.1029/90JB02237>.
- Mukasa, S.B., Andronikov, A., Brumley, K., Mayer, L.A., and Armstrong, A., 2020, Basalts from the Chukchi Borderland: ⁴⁰Ar/³⁹Ar ages and geochemistry of submarine intraplate lavas dredged from the western Arctic Ocean: *Journal of Geophysical Research*, *Solid Earth*, v. 125, no. 7, <https://doi.org/10.1029/2019JB017604>.
- Müller, R.D., Seton, M., Zahirovic, S., Williams, S.E., Matthews, K.J., Wright, N.M., Shephard, G.E., Maloney, K.T., Barnett-Moore, N., Hoesenpou, M., Bower, D.J., and Cannon, J., 2016, Ocean basin evolution and global-scale plate reorganization events since Pangea breakup: *Annual Review of Earth and Planetary Sciences*, v. 44, p. 107–138, <https://doi.org/10.1146/annurev-earth-060115-012211>.
- Müller, R.D., Zahirovic, S., Williams, S.E., Cannon, J., Seton, M., Bower, D.J., Tetley, M., Heine, C., Le Breton, E., Liu, S., Russell, S.H.J., Yang, T., Leonard, J., and Gurnis, M., 2019, A global plate model including lithospheric deformation along major rifts and orogens since the Triassic: *Tectonics*, v. 38, p. 1884–1907, <https://doi.org/10.1029/2018TC005462>.
- Murton, B.J., 1989, Tectonic controls on boninite genesis, in Saunders, A.D., and Norry, M.J., eds., *Magmatism in the Ocean Basins*: Geological Society of London, Special Publications, v. 42, p. 347–377, <https://doi.org/10.1144/GSL.SP.1989.042.01.20>.
- Ni, J.F., Guzman-Speziale, M., Bevis, M., Holt, W.E., Wallace, T.C., and Seager, W.R., 1989, Accretionary tectonics of Burma and the three-dimensional geometry of the Burma subduction zone: *Geology*, v. 17, p. 68–71, [https://doi.org/10.1130/0091-7613\(1989\)017<0068:ATOBAT>2.3.CO;2](https://doi.org/10.1130/0091-7613(1989)017<0068:ATOBAT>2.3.CO;2).
- Nicolas, A., and Boudier, F., 2017, Emplacement of Semail-Emirates ophiolite at ridge-trench collision: *Terra Nova*, v. 29, p. 127–134, <https://doi.org/10.1111/ter.12256>.
- Niu, X., Liu, F., Yang, J., Dilek, Y., Xu, Z., and Sein, K., 2017, Mineralogy, geochemistry, and melt evolution of the Kalaymyo peridotite massif in the Indo-Myanmar ranges (western Myanmar), and tectonic implications: *Lithosphere*, v. 10, p. 79–84, <https://doi.org/10.1130/L589.1>.
- Orme, D.A., Carrapa, B., and Kapp, P., 2015, Sedimentology, provenance and geochronology of the upper Cretaceous-lower Eocene western Xigaze forearc basin, southern Tibet: *Basin Research*, v. 27, p. 387–411, <https://doi.org/10.1111/bre.12080>.
- Parsioglu, N., Göhl, K., and Uenzelmann-Neben, G., 2008, The Agulhas Plateau: Structure and evolution of a Large Igneous Province: *Geophysical Journal International*, v. 174, p. 336–350, <https://doi.org/10.1111/j.1365-246X.2008.03808.x>.
- Patriat, M., Falloon, T., Danyushevsky, L., Collet, J., Jean, M.M., Hoernle, K., Maas, R., Woodhead, J.D., and Feig, S.T., 2019, Subduction initiation terranes exposed at the front of a 2 Ma volcanically-active subduction zone: *Earth and Planetary Science Letters*, v. 508, p. 30–40, <https://doi.org/10.1016/j.epsl.2018.12.011>.
- Peacock, S.M., Rushmer, T., and Thompson, A.B., 1994, Partial melting of subducting oceanic crust: *Earth and Planetary Science Letters*, v. 121, p. 227–244, [https://doi.org/10.1016/0012-821X\(94\)90042-6](https://doi.org/10.1016/0012-821X(94)90042-6).
- Pearce, J.A., 2008, Geochemical fingerprinting of oceanic basalts with applications to ophiolite classification and the search for Archean oceanic crust: *Lithos*, v. 100, p. 14–48, <https://doi.org/10.1016/j.lithos.2007.06.016>.
- Pearce, J.A., and Norry, M.J., 1979, Petrogenetic implications of Ti, Zr, Y, and Nb variations in volcanic rocks: Contributions to Mineralogy and Petrology, v. 69, p. 33–47, <https://doi.org/10.1007/BF00375192>.
- Pearce, J.A., and Peate, D.W., 1995, Tectonic implications of the composition of volcanic arc magmas: *Annual Review of Earth and Planetary Sciences*, v. 23, p. 251–285, <https://doi.org/10.1146/annurev.earth.23.050195.001343>.
- Pearce, J.A., Lippard, S.J., and Roberts, S., 1984, Characteristics and tectonic significance of supra-subduction zone ophiolites, in Kokelaar, B.P., and Howells, M.F., eds., *Marginal Basin Geology: Volcanic and Associated Sedimentary and Tectonic Processes in Modern and Ancient Marginal Basins*: Geological Society of London, Special Publications, v. 16, p. 77–94, <https://doi.org/10.1144/GSL.SP.1984.016.01.06>.
- Pearce, J.A., Van Der Laan, S.R., Arculus, R.J., Murton, B.J., Ishii, T., Peate, D.W., and Parkinson, I.J., 1992, Boninite and harzburgite from Leg 125 (Bonin-Mariana forearc): A case study of magma genesis during the initial stages of subduction: *Proceedings of the Ocean Drilling Program, Scientific Results*, v. 125, p. 623–659, <https://doi.org/10.2973/odp.proc.sr.125.172.1992>.
- Peccerillo, A., and Taylor, S.R., 1976, Geochemistry of Eocene calc-alkaline volcanic rocks from the Kastamonu area, northern Turkey: Contributions to Mineralogy and Petrology, v. 58, p. 63–81, <https://doi.org/10.1007/BF00384745>.
- Pedersen, R.B., Searle, M.P., Carter, A., and Bandopadhyay, P.C., 2010, U-Pb zircon age of the Andaman ophiolite: Implications for the beginning of subduction beneath the Andaman-Sumatra arc: *Journal of the Geological Society*, v. 167, p. 1105–1112, <https://doi.org/10.1144/0016-76492009-151>.
- Peterson, M.G., and Windley, B.F., 1991, Changing source regions of magmas and crustal growth in the Trans-Himalayas: Evidence from the Chalt Volcanics and Kohistan Batholith, Kohistan, northern Pakistan: *Earth and Planetary Science Letters*, v. 102, p. 326–341, [https://doi.org/10.1016/0012-821X\(91\)90027-F](https://doi.org/10.1016/0012-821X(91)90027-F).
- Plank, T., 2005, Constraints from thorium/lanthanum on sediment recycling at subduction zones and the evolution of the continents: *Journal of Petrology*, v. 46, p. 921–944, <https://doi.org/10.1093/ptrology/egi005>.
- Plummer, P.S., 1996, The Amirante ridge/trough complex: Response to rotational transform rift drift between Seychelles and Madagascar: *Terra Nova*, v. 8, p. 34–47, <https://doi.org/10.1111/j.1365-3121.1996.tb00723.x>.
- Plunder, A., Bandyopadhyay, D., Ganerød, M., Advokaat, E.L., Ghosh, B., Bandopadhyay, P., and Hinsbergen, D.J.J., 2020, History of subduction polarity reversal during arc-continent collision: Constraints from the Andaman ophiolite and its metamorphic sole: *Tectonics*, v. 39, no. 6, <https://doi.org/10.1029/2019TC005762>.
- Poinar, J.G., 2019, Burmese amber: evidence of Gondwanan origin and Cretaceous dispersion: *Historical Biology*, v. 31, no. 10, p. 1304–1309, <https://doi.org/10.1080/08912963.2018.1446531>.
- Proust, F., Burg, J.P., Matte, P., Tapponnier, P., Li, T., Li, G., and Chen, G., 1984, Succession des phases de plissement sur une transversale du Tibet meridional, implication géodynamiques, in Mercier, J.L., and Li, G.C., eds., *Mission Franco-Chinoise au Tibet 1980. Étude géologique et géophysique de la croûte terrestre et du manteau supérieur du Tibet et de l'Himalaya*: Paris, France, Centre National de la Recherche Scientifique, p. 385–392.
- Qian, Q., Hermann, J., Dong, F., Lin, L., and Sun, B., 2020, Episodic formation of Neotethyan ophiolites (Tibetan plateau): Snapshots of abrupt global plate reorganizations during major episodes of supercontinent breakup?: *Earth-Science Reviews*, v. 203, no. 103144, <https://doi.org/10.1016/j.earscirev.2020.103144>.
- Reagan, M.K., Ishizuka, O., Stern, R.J., Kelley, K.A., Ohara, Y., Blichert-Toft, J., Bloomer, S.H., Cash, J.,

- Fryer, P., Hanan, B.B., Hickey-Vargas, R., Ishii, T., Kimura, J.-I., Peate, D.W., Rowe, M.C., and Woods, M., 2010, Fore-arc basalts and subduction initiation in the Izu-Bonin-Mariana system: *Geochemistry, Geophysics, Geosystems*, v. 11, no. 3, <https://doi.org/10.1029/2009GC002871>.
- Reagan, M.K., Pearce, J.A., Petronotis, K., Almeev, R., Avery, A.J., and Carvallo, C., Chapman, T., Christeson, G.L., Ferré, E.C., Godard, M., Heaton, D.E., Kirchenbaur, M., Kurz, W., Kutterolf, S., Hongyan, L., Yibing, L., Michibayashi, K., Morgan, S., Nelson, W.R., Prytulak, J., Python, M., Robertson, A.H.F., Ryan, J.G., Sager, W.W., Sakuyama, T., Shervais, J.W., Shimizu, K., and Whattam, S.A., 2015, Expedition 352 summary: Proceedings of the International Ocean Discovery Program, v. 352, p. 1–32, <https://doi.org/10.14379/iodp.proc.352.102.2015>.
- Reagan, M.K., Heaton, D.E., Schmitz, M.D., Pearce, J.A., Shervais, J.W., and Koppers, A.A.P., 2019, Forearc ages reveal extensive short-lived and rapid seafloor spreading following subduction initiation: *Earth and Planetary Science Letters*, v. 506, p. 520–529, <https://doi.org/10.1016/j.epsl.2018.11.020>.
- Reay, A., and Parkinson, D., 1997, Adakites from Solander Island, New Zealand: *New Zealand Journal of Geology and Geophysics*, v. 40, p. 121–126, <https://doi.org/10.1080/00288306.1997.9514746>.
- Sarma, D.S., Jafri, S.H., Fletcher, I.R., and McNaughton, N.J., 2010, Constraints on the tectonic setting of the Andaman ophiolites, Bay of Bengal, India, from SHRIMP U-Pb zircon geochronology of plagiogranite: *The Journal of Geology*, v. 118, p. 691–697, <https://doi.org/10.1086/656354>.
- Schmidt, M.W., and Jagoutz, O., 2017, The global systematics of primitive arc melts: *Geochemistry, Geophysics, Geosystems*, v. 18, p. 2817–2854, <https://doi.org/10.1002/2016GC006699>.
- Searle, M.P., Windley, B.F., Coward, M.P., Cooper, D.J.W., Rex, A.J., and Li, T.D., 1987, The closing of Tethys and the tectonics of the Himalaya: *Geological Society of America Bulletin*, v. 98, p. 678–701, [https://doi.org/10.1130/0016-7606\(1987\)98<678:TCOTAT>2.0.CO;2](https://doi.org/10.1130/0016-7606(1987)98<678:TCOTAT>2.0.CO;2).
- Searle, M.P., Khan, M.A., Fraser, J.E., Gough, S.J., and Jan, M.Q., 1999, The tectonic evolution of the Kohistan-Karakoram collision belt along the Karakoram Highway transect, north Pakistan: *Tectonics*, v. 18, p. 929–949, <https://doi.org/10.1029/1999TC900042>.
- Searle, M.P., Noble, S.R., Cottle, J.M., Waters, D.J., Mitchell, A.H.G., Hlaing, T., and Horstwood, M.S.A., 2007, Tectonic evolution of the Mogok metamorphic belt, Burma (Myanmar) constrained by U-Th-Pb dating of metamorphic and magmatic rocks: *Tectonics*, v. 26, no. 3, <https://doi.org/10.1029/2006TC002083>.
- Searle, M.P., Waters, D.J., Garber, J.M., Rioux, M., Cherry, A.G., and Ambrose, T.K., 2015, Structure and metamorphism beneath the obducting Oman ophiolite: Evidence from the Bani Hamid granulites, northern Oman mountains: *Geosphere*, v. 11, no. 6, p. 1812–1836, <https://doi.org/10.1130/GES01199.1>.
- Seton, M., Müller, R.D., Zahirovic, S., Gaina, C., Torsvik, T., Shephard, G., Talsma, A., Gurnis, M., Turner, M., Maus, S., and Chandler, M., 2012, Global continental and ocean basin reconstructions since 200 Ma: *Earth-Science Reviews*, v. 113, p. 212–270, <https://doi.org/10.1016/j.earscirev.2012.03.002>.
- Sevastjanova, I., Hall, R., Rittner, M., Paw, S.M.T.L., Nang, T.T., Alderton, D.H., and Comfort, G., 2016, Myanmar and Asia united, Australia left behind long ago: *Gondwana Research*, v. 32, p. 24–40, <https://doi.org/10.1016/j.gr.2015.02.001>.
- Seyfried, W.E., and Mottl, M.J., 1982, Hydrothermal alteration of basalt by sea-water under seawater-dominated conditions: *Geochimica et Cosmochimica Acta*, v. 46, p. 985–1002, [https://doi.org/10.1016/0016-7037\(82\)90054-0](https://doi.org/10.1016/0016-7037(82)90054-0).
- Shervais, J.W., 1982, Ti-V plots and the petrogenesis of modern and ophiolitic lavas: *Earth and Planetary Science Letters*, v. 59, p. 101–118, [https://doi.org/10.1016/0012-821X\(82\)90120-0](https://doi.org/10.1016/0012-821X(82)90120-0).
- Shervais, J.W., 2001, Birth, death, and resurrection: The life cycle of suprasubduction zone ophiolites: *Geochemistry, Geophysics, Geosystems*, v. 2, no. 1, <https://doi.org/10.1029/2000GC000080>.
- Shervais, J.W., Reagan, M., Haugen, E., Almeev, R.R., Pearce, J.A., Prytulak, J., Ryan, J.G., Whattam, S.A., Godard, M., Chapman, T., Li, H., Kurz, W., Nelson, W.R., Heaton, D., Kirchenbaur, M., Shimizu, K., Sakuyama, T., Li, Y., and Vetter, S.K., 2019, Magmatic response to subduction initiation: Part 1. Fore-arc basalts of the Izu-Bonin Arc from IODP Expedition 352: *Geochemistry, Geophysics, Geosystems*, v. 20, p. 314–338, <https://doi.org/10.1029/2018GC007731>.
- Shi, G.H., Grimaldi, D.A., Harlow, G.E., Wang, J., Wang, J., Yang, M.C., Lei, W.Y., Li, Q.L., and Li, X.H., 2012, Age constraint on Burmese amber based on U-Pb dating of zircons: *Cretaceous Research*, v. 37, p. 155–163, <https://doi.org/10.1016/j.cretres.2012.03.014>.
- Sláma, J., Košler, J., Condon, D.J., Crowley, J.L., Gerdes, A., Hancher, J.M., Horstwood, M.S.A., Morris, G.A., Nasdala, L., Norberg, N., Schaltegger, U., Schoene, B., Tubrett, M.N., and Whitehouse, M.J., 2008, Plešovice zircon: A new natural reference material for U-Pb and Hf isotopic microanalysis: *Chemical Geology*, v. 249, p. 1–35, <https://doi.org/10.1016/j.chemgeo.2007.11.005>.
- Smith, D.K., Cann, J.R., and Escartín, J., 2006, Widespread active detachment faulting and core complex formation near 13° N on the Mid-Atlantic Ridge: *Nature*, v. 442, p. 440–443, <https://doi.org/10.1038/nature04950>.
- Sloan, R.A., Elliott, J.R., Searle, M.P., and Morley, C.K., 2017, Active tectonics of Myanmar and the Andaman Sea, in Barber, A.J., Khin, Z., and Crow, M.J., eds., Myanmar: *Geology, Resources and Tectonics*: Geological Society of London Memoirs, v. 48, p. 19–52, <https://doi.org/10.1144/M48.2>.
- Soret, M., Agard, P., Dubacq, B., Plunder, A., and Yamato, P., 2017, Petrological evidence for stepwise accretion of metamorphic soles during subduction infancy (Semail ophiolite, Oman and UAE): *Journal of Metamorphic Geology*, v. 35, p. 1051–1080, <https://doi.org/10.1111/jmg.12267>.
- Staudigel, H., and Hart, S.R., 1983, Alteration of basaltic glass-mechanisms and significance for the oceanic-crust seawater budget: *Geochimica et Cosmochimica Acta*, v. 47, p. 337–350, [https://doi.org/10.1016/0016-7037\(83\)90257-0](https://doi.org/10.1016/0016-7037(83)90257-0).
- Stern, R.J., 2002, Subduction zones: *Reviews of Geophysics*, v. 40, no. 4, <https://doi.org/10.1029/2001RG000108>.
- Stern, R.J., 2004, Subduction initiation: Spontaneous and induced: *Earth and Planetary Science Letters*, v. 226, p. 275–292, [https://doi.org/10.1016/S0012-821X\(04\)00498-4](https://doi.org/10.1016/S0012-821X(04)00498-4).
- Stern, R.J., and Bloomer, S.H., 1992, Subduction zone infancy: Examples from the Eocene Izu-Bonin-Mariana and Jurassic California arcs: *Geological Society of America Bulletin*, v. 104, p. 1621–1636, [https://doi.org/10.1130/0016-7606\(1992\)104<1621:SZIEFT>2.3.CO;2](https://doi.org/10.1130/0016-7606(1992)104<1621:SZIEFT>2.3.CO;2).
- Stern, R.J., and Gerya, T., 2018, Subduction initiation in nature and models: A review: *Tectonophysics*, v. 746, p. 173–198, <https://doi.org/10.1016/j.tecto.2017.10.014>.
- Sutherland, R., Barnes, P., and Uruski, C., 2006, Miocene-Recent deformation, surface elevation, and volcanic intrusion of the overriding plate during subduction initiation, offshore southern Fiordland, Puysegur margin, southwest New Zealand: *New Zealand Journal of Geology and Geophysics*, v. 49, p. 131–149, <https://doi.org/10.1080/00288306.2006.9515154>.
- Syracuse, E.M., and Abers, G.A., 2006, Global compilation of variations in slab depth beneath arc volcanoes and implications: *Geochemistry, Geophysics, Geosystems*, v. 7, no. 5, <https://doi.org/10.1029/2005GC001045>.
- Syracuse, E.M., van Keken, P.E., and Abers, G.A., 2010, The global range of subduction zone thermal models: Physics of the Earth and Planetary Interiors, v. 183, p. 73–90, <https://doi.org/10.1016/j.pepi.2010.02.004>.
- Teagle, D.A.H., and Alt, J.C., 2004, Hydrothermal alteration of basalts beneath the Bent Hill massive sulfide deposit, Middle Valley, Juan de Fuca Ridge: *Economic Geology and the Bulletin of the Society of Economic Geologists*, v. 99, p. 561–584, <https://doi.org/10.2113/gsecongeo.99.3.561>.
- Toth, J., and Gurnis, M., 1998, Dynamics of subduction initiation at preexisting fault zones: *Journal of Geophysical Research*, v. 103, p. 18053–18067, <https://doi.org/10.1029/98JB01076>.
- Ulvrova, M.M., Brune, S., and Williams, S., 2019, Breakup without borders: How continents speed up and slow down during rifting: *Geophysical Research Letters*, v. 46, p. 1338–1347, <https://doi.org/10.1029/2018GL080387>.
- Umino, S., Kitamura, K., Kanayama, K., Tamura, A., Sakamoto, N., Ishizuka, O., and Arai, S., 2015, Thermal and chemical evolution of the subarc mantle revealed by spinel-hosted melt inclusions in boninite from the Ogasawara (Bonin) Archipelago, Japan: *Geology*, v. 43, p. 151–154, <https://doi.org/10.1130/G36191.1>.
- van Hinsberger, D.J.J., Steinberger, B., Doubrovine, P.V., and Gassmüller, R., 2011, Acceleration and deceleration of India-Asia convergence since the Cretaceous: Roles of mantle plumes and continental collision: *Journal of Geophysical Research*, v. 116, <https://doi.org/10.1029/2010JB008051>.
- van Hinsberger, D.J.J., Peters, K., Maffione, M., Spakman, W., Guilmette, C., Thieulot, C., Thieulot, C., Plümper, O., Güler, D., Brouwer, F.M., Aldanmaz, E., and Kaymakci, N., 2015, Dynamics of intraoceanic subduction initiation: 2. Suprasubduction zone ophiolite formation and metamorphic sole exhumation in context of absolute plate motions: *Geochemistry, Geophysics, Geosystems*, v. 16, p. 1771–1785, <https://doi.org/10.1002/2015GC005745>.
- van Hinsberger, D.J.J., Maffione, M., Plunder, A., Kaymakci, N., Ganevod, M., Hendriks, B.W.H., Corfu, F., Güler, D., de Gelder, G.I.N.O., Peters, K., McPhee, P.J., Brouwer, F.M., Advokaat, E.L., and Vissers, R.L.M., 2016, Tectonic evolution and paleogeography of the Kirşehir Block and the Central Anatolian Ophiolites, Turkey: *Tectonics*, v. 35, no. 4, p. 983–1014, <https://doi.org/10.1002/2015TC004018>.
- van Hinsbergen, D.J.J., Torsvik, T.H., Schmid, S.M., Mañenco, L.C., Maffione, M., Vissers, R.L.M., Güler, D., and Spakman, W., 2020, Orogenic architecture of the Mediterranean region and kinematic reconstruction of its tectonic evolution since the Triassic: *Gondwana Research*, v. 81, p. 79–229, <https://doi.org/10.1016/j.jgr.2019.07.009>.
- Vigny, C., Socquet, A., Rangin, C., Chamotrooke, N., Pubellier, M., Bouin, M.N., Bertrand, G., and Becker, M., 2003, Present-day crustal deformation around Sagaing fault, Myanmar: *Journal of Geophysical Research*, v. 108, <https://doi.org/10.1029/2002jb001999>.
- Wakabayashi, J., and Dilek, Y., 2000, Spatial and temporal relationships between ophiolites and their metamorphic soles: A test of models of forearc ophiolite genesis, in Dilek, Y., Moores, E.M., Elthon, D., and Nicolas, A., eds., *Ophiolites and Oceanic Crust: New Insights from Field Studies and the Ocean Drilling Program*: Geological Society of America Special Paper 349, 53–64, <https://doi.org/10.1130/0-8137-2349-3.53>.
- Wang, J.G., Wu, F.Y., Tan, X.C., and Liu, C.Z., 2014, Magmatic evolution of the Western Myanmar Arc documented by U-Pb and Hf isotopes in detrital zircon: *Tectonophysics*, v. 612, p. 97–105, <https://doi.org/10.1016/j.tecto.2013.11.039>.
- Wang, J.G., Hu, X., Garzanti, E., An, W., and Liu, X.-C., 2017a, The birth of the Xigaze forearc basin in southern Tibet: *Earth and Planetary Science Letters*, v. 465, p. 38–47, <https://doi.org/10.1016/j.epsl.2017.02.036>.
- Wang, Y., Huang, X., Sun, Y., Zhao, S., and Yue, Y., 2017b, A new method for the separation of LREEs in geological materials using a single TODGA resin column and its application to the determination of Nd isotope compositions by MC-ICPMS: *Analytical Methods*, v. 9, p. 3531–3540, <https://doi.org/10.1039/C7AY00966F>.
- Westerweel, J., Roperch, P., Licht, A., Dupont-Nivet, G., Win, Z., Poblete, F., Ruffet, G., Swe, H.H., Thi, M.K., and Aung, D.W., 2019, Burma Terrane part of the Trans-Tethyan arc during collision with India according to palaeomagnetic data: *Nature Geoscience*, v. 12, p. 863–868, <https://doi.org/10.1038/s41561-019-0443-2>.
- Westerweel, J., Licht, A., Cogné, N., Roperch, P., Dupont-Nivet, G., Kay Thi, M., Swe, H.H., Huang, H., Win, Z., and Wa Aung, D., 2020, Burma Terrane collision and northward indentation in the eastern Himalayas

- recorded in the Eocene-Miocene Chindwin Basin (Myanmar): *Tectonics*, v. 39, no. 10, <https://doi.org/10.1029/2020TC006413>.
- Wiedenbeck, M., Hanchar, J.M., Peck, W.H., Sylvester, P., Valley, J., Whitehouse, M., Kronz, A., Morishita, Y., Nasdala, L., Fiebig, J., Franchi, I., Girard, J.P., Greenwood, R.C., Hinton, R., Kita, N., Mason, P.R.D., Norman, M., Ogasawara, M., Piccoli, R., Rhede, D., Satoh, H., Schulz-Dobrick, B., Skar, O., Spicuzza, M.J., Terada, K., Tindle, A., Togashi, S., Vennemann, T., Xie, Q., and Zheng, Y.F., 2004, Further characterisation of the 91500 zircon crystal: *Geostandards and Geoanalytical Research*, v. 28, p. 9–39, <https://doi.org/10.1111/j.1751-908X.2004.tb01041.x>.
- Xie, J.-C., Zhu, D.-C., Dong, G., Zhao, Z.-D., Wang, Q., and Mo, X., 2016, Linking the Tengchong Terrane in SW Yunnan with the Lhasa Terrane in southern Tibet through magmatic correlation: *Gondwana Research*, v. 39, p. 217–229, <https://doi.org/10.1016/j.gr.2016.02.007>.
- Xiong, Q., Griffin, W.L., Zheng, J.-P., O'Reilly, S.Y., Pearson, N.J., Xu, B., and Belousova, E.A., 2016, Southward trench migration at ~130–120 Ma caused accretion of the Neo-Tethyan forearc lithosphere in Tibetan ophiolites: *Earth and Planetary Science Letters*, v. 438, p. 57–65, <https://doi.org/10.1016/j.epsl.2016.01.014>.
- Yajima, K., and Fujimaki, H., 2001, High-Ca and low-Ca boninites from Chichijima, Bonin (Ogasawara) archipelago: *Japanese Magazine of Mineralogical and Petrological Sciences*, v. 30, p. 217–236, <https://doi.org/10.2465/gkk.30.217>.
- Yang, J.S., Xu, Z.Q., Duan, X.D., Li, J., Xiong, F.H., Liu, Z., Cai, Z.H., and Li, H.Q., 2012, Discovery of a Jurassic SSZ ophiolite in the Myitkyina region of Myanmar [in Chinese with English abstract]: *Acta Petrologica Sinica*, v. 28, p. 1710–1730.
- Yao, W., Ding, L., Cai, F.L., Wang, H.Q., Xu, Q., and Zaw, T., 2017, Origin and tectonic evolution of upper Triassic Turbidites in the Indo-Burman ranges, West Myanmar: *Tectonophysics*, v. 721, p. 90–105, <https://doi.org/10.1016/j.tecto.2017.09.016>.
- Yogodzinski, G.M., Bizimis, M., Hickey-Vargas, R., McCarthy, A., Hocking, B.D., Savov, I.P., Shizuka, O., and Arculus, R., 2018, Implications of Eocene-age Philippine Sea and forearc basalts for initiation and early history of the Izu-Bonin-Mariana arc: *Geochimica et Cosmochimica Acta*, v. 228, p. 136–156, <https://doi.org/10.1016/j.gca.2018.02.047>.
- Zahirovic, S., Matthews, K.J., Flament, N., Müller, R.D., Hill, K.C., Seton, M., and Gurnis, M., 2016, Tectonic evolution and deep mantle structure of the eastern Tethys since the latest Jurassic: *Earth-Science Reviews*, v. 162, p. 293–337, <https://doi.org/10.1016/j.earscirev.2016.09.005>.
- Zaman, H., and Torii, M., 1999, Palaeomagnetic study of Cretaceous red beds from the eastern Hindukush ranges, northern Pakistan: Palaeoreconstruction of the Kohistan-Karakoram composite unit before the India-Asia collision: *Geophysical Journal International*, v. 136, p. 719–738, <https://doi.org/10.1046/j.1365-246x.1999.00757.x>.
- Zhang, C., Liu, C.Z., Xu, Y., Ji, W.B., Wang, J.M., Wu, F.Y., Liu, T., Zhang, Z.Y., and Zhang, W.Q., 2019a, Subduction re-initiation at dying ridge of Neo-Tethys: Insights from mafic and metamafic rocks in Lhaze ophiolitic melange, Yarlung-Tsangbo Suture Zone: *Earth and Planetary Science Letters*, v. 523, no. 115707, <https://doi.org/10.1016/j.epsl.2019.07.009>.
- Zhang, G., He, Y., Ai, Y., Jiang, M., Mon, C.T., Hou, G., Thant, M., and Sein, K., 2021, Indian continental lithosphere and related volcanism beneath Myanmar: Constraints from local earthquake tomography: *Earth and Planetary Science Letters*, v. 567, <https://doi.org/10.1016/j.epsl.2021.116987>.
- Zhang, J.E., Xiao, W.J., Windley, B., Cai, F.L., Sein, K., and Naing, S., 2017a, Early Cretaceous wedge extrusion in the Indo-Burma Range accretionary complex: Implications for the Mesozoic subduction of Neotethys in SE Asia: *International Journal of Earth Sciences*, v. 106, p. 1391–1408, <https://doi.org/10.1007/s00531-017-1468-7>.
- Zhang, J.E., Xiao, W., Windley, B. F., Wakabayashi, J., Cai, F., Sein, K., Wu, H., Naing, S., 2018, Multiple alternating forearc- and backarc-ward migration of magmatism in the Indo-Myanmar Orogenic Belt since the Jurassic: Documentation of the orogenic architecture of eastern Neotethys in SE Asia: *Earth-Science Reviews*, v. 185, p. 704–731, <https://doi.org/10.1016/j.earscirev.2018.07.009>.
- Zhang, L.Y., Ducea, M.N., Ding, L., Pullen, A., Kapp, P., and Hoffman, D., 2014, Southern Tibetan Oligocene-Miocene adakites: A record of Indian slab tearing: *Lithos*, v. 210, p. 209–223, <https://doi.org/10.1016/j.lithos.2014.09.029>.
- Zhang, L.Y., Fan, W.M., Ding, L., Ducea, M.N., Pullen, A., Li, J.X., Sun, Y.L., Yue, Y.H., Cai, F.L., Wang, C., Peng, T.P., and Sein, K., 2020, Quaternary volcanism in Myanmar: A record of Indian slab tearing in a transition zone from oceanic to continental subduction: *Geochemistry, Geophysics, Geosystems*, v. 21, no. 8, <https://doi.org/10.1029/2020GC009091>.
- Zhang, P., Mei, L.F., Hu, X.L., Li, R.Y., Wu, L.L., Zhou, Z.C., and Qiu, H.N., 2017b, Structures, uplift, and magmatism of the Western Myanmar Arc: Constraints to mid-Cretaceous–Paleogene tectonic evolution of the western Myanmar continental margin: *Gondwana Research*, v. 52, p. 18–38, <https://doi.org/10.1016/j.gr.2017.09.002>.
- Zhang, S.-Q., Mahoney, J., Mo, X.-X., Ghazi, A., Milani, L., Crawford, A., Guo, T.-Y., and Zhao, Z.-D., 2005, Evidence for a widespread Tethyan upper mantle with Indian-Ocean-type isotopic characteristics: *Journal of Petrology*, v. 46, p. 829–858, <https://doi.org/10.1093/petrology/egi002>.
- Zhang, X.R., Chung, S.L., Lai, Y.M., Ghani, A.A., Murtadha, S., Lee, H.Y., and Hsu, C.C., 2019b, A 6000-km-long Neo-Tethyan arc system with coherent magmatic flare-ups and lulls in South Asia: *Geology*, v. 47, p. 573–576, <https://doi.org/10.1130/G46172.1>.
- Zheng, T., He, Y., Ding, L., Jiang, M., Ai, Y., Mon, C.T., Hou, G., Sein, K., and Thant, M., 2020, Direct structural evidence of Indian continental subduction beneath Myanmar: *Nature Communications*, v. 11, no. 1, <https://doi.org/10.1038/s41467-020-15746-3>.

SCIENCE EDITOR: BRAD S. SINGER
ASSOCIATE EDITOR: XIXI ZHAO

MANUSCRIPT RECEIVED 5 JULY 2020
REVISED MANUSCRIPT RECEIVED 7 MAY 2021
MANUSCRIPT ACCEPTED 27 MAY 2021

Printed in the USA